6 Nanocomposites Based on POSS

Shiao-Wei Kuo[1], *Chih-Feng Huang*[2], *and Feng-Chih Chang*[2]

[1]Department of Materials Science and Optoelectronic Engineering, Center for Nanoscience and Nanotechnology, National Sun Yat-Sen University, Kaohsiung, Taiwan

[2]Institute of Applied Chemistry, National Chiao-Tung University, Hsin-Chu, Taiwan

changfc@mail.nctu.edu.tw

Abstract

This chapter describes in detail the synthesis of polyhedral oligomeric silsesquioxane (POSS) compounds, the miscibility of POSS derivatives and polymers, and the preparation of monomers and polymers containing POSS, including styryl-POSS, methacrylate-POSS, norbornyl-POSS, vinyl-POSS, epoxy-POSS, phenolic-POSS, benzoxazine-POSS, amine-POSS, and hydroxyl-POSS. Both monofunctional and multifunctional monomers are used in commercial and/or high-performance thermoplastic and thermosetting polymers, the corresponding thermal, dynamic mechanical, electrical, and surface properties are also discussed in detail herein.

6.1. Introduction

The field of polymer nanocomposite materials has attracted great attention, imagination, and interest from polymer scientists and engineers in recent years. The simple premise of using building blocks having nanosize dimensions makes it possible to create new polymeric materials exhibiting improved physical properties, such as unprecedented flexibility. Silsesquioxanes are nanostructures having the empirical formula $RSiO_{1.5}$, where R is a hydrogen atom or an organic functional group, such as an alkyl, alkylene, acrylate, hydroxyl, or epoxide unit. Figure 6.1 illustrates the silsesquioxanes that may be formed from random, ladder, cage, and partial cage structures [1].

In 1946, Scott et al. discovered the first oligomeric organosilsesquioxane, $(CH_3SiO_{1.5})_n$, along with other volatile compounds through the thermolysis of polymeric products prepared from the methyl trichlorosilane and dimethyl chlorosilane co-hydrolysis method [2]. Interest in this field has increased dramatically in recent years, even though silsequioxane chemistry has been studied for more than half a century. In 1995, Baney et al. [3] reviewed the preparation, properties, structures, and applications of silsequioxanes, especially those of the ladder-like polysilsesquioxanes (Figure 6.1(b)). These ladder-like structures display excellent thermal stability, oxidative resistance at temperatures greater than 500°C, and good insulating and gas permeability properties [4]. More recently, attention has been concentrated on silsesquioxanes possessing the specific cage structures displayed in Figures 6.1(c)–(f). These polyhedral oligomeric silsesquioxanes are commonly abbreviated

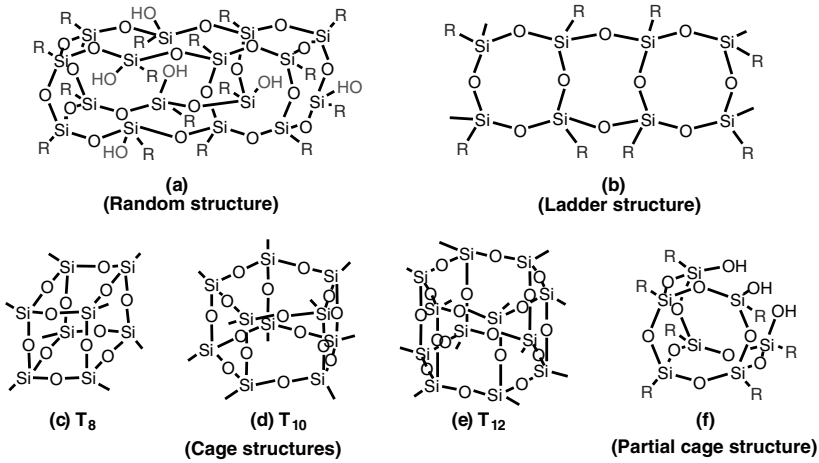

Figure 6.1 Structures of silsesquioxanes.

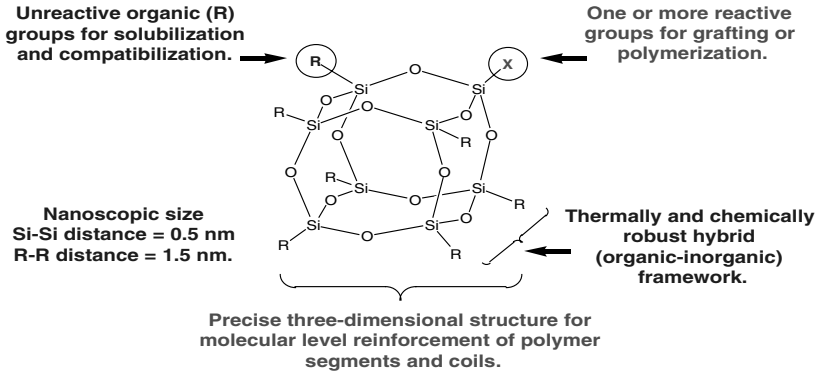

Figure 6.2 Chemical structure of POSS.

as "POSS." POSS compounds are true hybrid inorganic/organic chemical composites that possess an inner inorganic silicon and oxygen core $(SiO_{1.5})_n$ and external organic substituents that can possess a range of polar and nonpolar structures and functional groups.

Figure 6.2 displays POSS nanostructures having diameters ranging from 1 to 3 nm; they can be considered as the smallest possible particles of silica, i.e., molecular silica. Unlike most silicones or fillers, POSS molecules containing organic substituents on their outer surfaces are compatible or miscible with most polymers. In addition, these functional groups can be specially designed as either nonreactive or reactive to be used in polymer blending or copolymerization. POSS derivatives have been prepared with one or more covalently bonded reactive functionalities so that they become suitable for polymerization, grafting, surface bonding, or other transformations. Unlike traditional organic compounds, POSS derivatives release no volatile organic components; thus, they are odorless and environmentally friendly materials. The incorporation of POSS moieties into polymeric materials can dramatically improve the polymers' properties (e.g., strength, modulus, rigidity) as well as reduce flammability, heat evolution, and viscosity during processing. These enhancements

apply to a wide range of commercial thermoplastic polymers (e.g., PE, PP, PS, PMMA, PEO, and PCL), high-performance thermoplastic polymers (e.g., polyimide and PLED), and thermosetting polymers (e.g., epoxy resin, phenolic resin, and polybenzoxazine). It is especially convenient to incorporate the POSS moieties into polymers through simple blending or copolymerization. In addition, when POSS monomers are soluble in monomer mixtures, they can be incorporated as true molecular dispersions in copolymer systems. The macrophase separation that usually occurs through the aggregation of POSS units can be avoided through copolymerization (i.e., as a result of covalent bond formation between POSS and polymers) – a significant advantage over current filler technologies. POSS nanostructures also have significant promise for use in catalyst supports and biomedical applications, such as scaffolds for drug delivery, imaging reagents, and combinatorial drug development.

In this chapter, we describe methods for synthesizing POSS compounds and preparing monomers and polymers containing POSS. We discuss the monofunctional and multifunctional POSS monomers that have been used for thermoplastic and thermosetting polymers. In addition, we compare the miscibility, phase behavior, thermal, dynamic mechanical, electric, and surface properties of polymers containing POSS.

6.2. General Approaches Toward Synthesizing Polyhedral Oligomeric Silsesquioxanes

POSS derivatives feature Si–O linkages in the form of a cage presenting a silicon atom at each vertex, with substituents coordinating around the silicon vertices tetrahedrally. The nature of the exo cage substituent in such compounds determines the mechanical, thermal, and other physical properties. The number of $RSiO_3$ units determines the shape of the frame, which is uniquely unstrained for 6 to 12 units. A review by Voronkov et al. published in 1982 covered the known methods of synthesizing POSS compounds [5]. In 2000, Feher and co-workers reviewed recent progress in the field of POSS synthesis [6]. There are many substituents appended to the silicon/oxygen cages $(RSiO_{1.5})_n$ (where R is an organic or inorganic group; Figure 6.3) that are suitable for polymerization or copolymerization

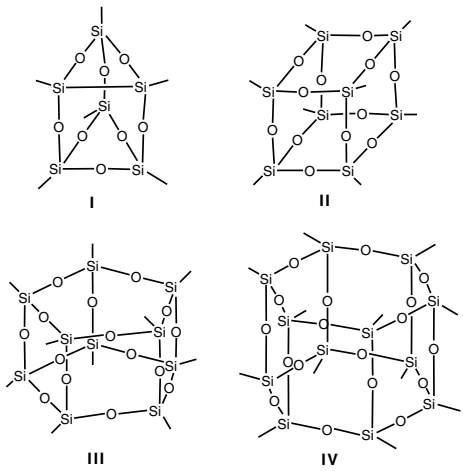

Figure 6.3 Cage structures of POSS where T_6(I), T_8(II), T_{10}(III), and T_{12}(IV).

between the specific POSS derivative with other monomers. The general methods of synthesizing both monofunctional and multifunctional octahedral silsesquioxanes (T_8), and examples of such derivatives, are described briefly below.

6.2.1. Monofunctional POSS

Monofunctional POSS derivatives are among the most useful compounds for polymerization or copolymerization with other monomers. Figure 6.4 summarizes the three general approaches toward synthesizing monofunctional POSS derivatives of the form $R'R_7Si_8O_{12}$.

Route I. Co-hydrolysis of trifunctional organo- or hydrosilanes: Polycondensation of monomers is the classical method of synthesizing silsesquioxanes. When this reaction is performed in the presence of monomers possessing various R groups, mixtures of heterosubstituted compounds are obtained, including the desired monosubstituted products [7, 8].

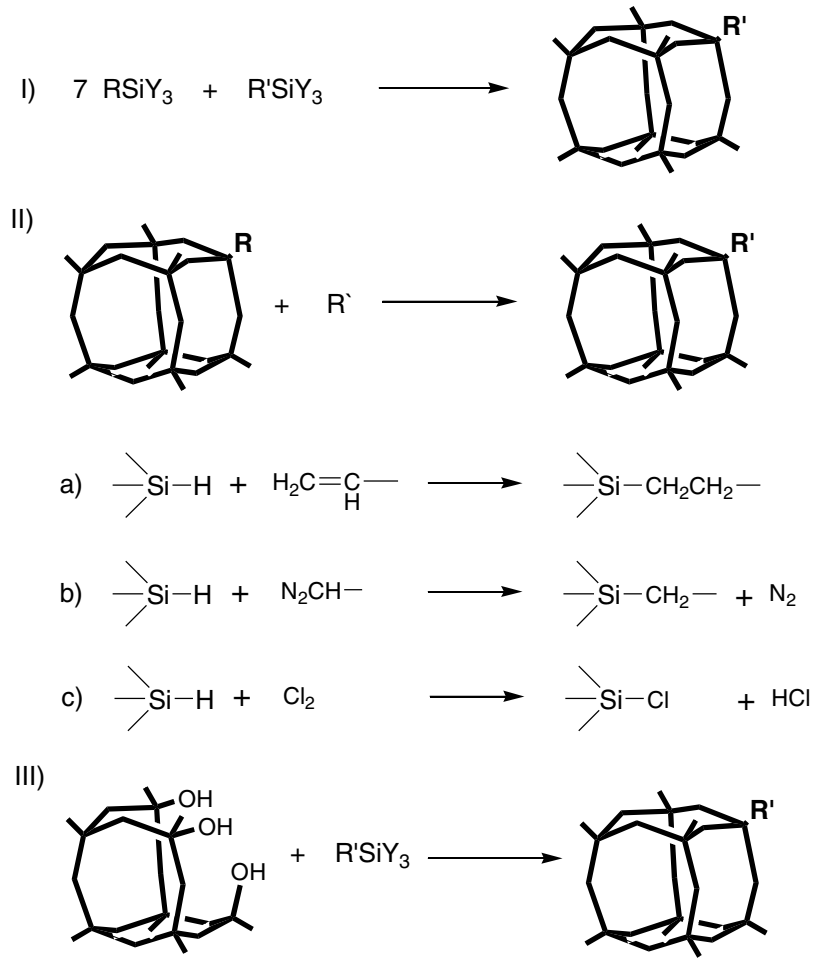

Figure 6.4 Three general ways of synthesizing monosubstituted octasilasesquioxane.

Route II. Substitution reactions with retention of the siloxane cage: Figure 6.4 presents a selection of substitution reactions using octahydro-silsesquioxane as starting materials (IIa–c) that have been applied successfully to prepare monosubstituted silsesquioxanes. By adjusting the ratio of the reactants, it is possible to obtain a considerable yield of the desired monosubstituted product [9–14].

Route III. Corner-capping reactions: Feher and co-workers developed this approach starting from the incompletely condensed $R_7Si_7O_9(OH)_3$ molecules (T_7) [15–18]. The three silanol groups are very reactive toward $RSiCl_3$, giving the fully condensed products. Variation of the R group on the silane enables the syntheses of a variety of monofunctionalized siloxane cages [19, 20]. Subsequent transformations can be performed until the desired functionality is obtained. Moreover, incompletely condensed silsesquioxanes offer a route toward the generation of hetero- and metalla-siloxanes in which a hetero main group or a transition metal element is introduced into the silicon–oxygen framework [15–17, 21–24].

6.2.2. Multifunctional POSS

POSS $(RSiO_{1.5})_n$ derivatives in which R is a hydrogen atom and the value of n is 8, 10, or 12 are unique structures generally formed through hydrolysis and condensation of trialkoxysilanes [$HSi(OR)_3$] or trichlorosilanes ($HSiCl_3$) [5]. The hydrolysis of trimethoxysilane in cyclohexane/acetic acid mixtures in the presence of concentrated hydrochloric acid provides the octamer in low yield (13%) [25]. The hydrolytic polycondensation of trifunctional monomers of the type $RSiY_3$ leads to crosslinked three-dimensional networks and *cis*-syndiotactic (ladder-type) polymers, $(RSiO_{1.5})_n$. The reaction rates, degrees of oligomerization, and yields of the polyhedral compounds formed under these conditions are strongly dependent on several factors, including the concentration of the initial monomer in the solution, the nature of the solvent, the identity of the substituent R, the functional group Y in the initial monomer, the type of catalyst, the reaction temperature, the rate of addition of water, and the solubility of the polyhedral oligomers formed [25]. For example, POSS cages in which n is 4 or 6 can be obtained in nonpolar or weakly polar solvents at 0°C or 20°C, but not in alcohols. In contrast, octa(phenylsilsesquioxane) $[Ph_8(SiO_{1.5})_8]$ is more readily formed in benzene, nitrobenzene, benzyl alcohol, pyridine, or ethylene glycol dimethyl ether at high temperature (e.g., 100°C). The effects of each of these factors affecting POSS synthesis have been reviewed in depth previously [25]. Another approach toward multifunctional POSS derivatives is the functionalizing of preformed POSS cages; e.g., through Pt-catalyzed hydrosilylation of alkenes or alkynes with $(HSiO_{1.5})_8$ and $(HMe_2SiOSiO_{1.5})_8$ cages (Figure 6.5) [26–28].

6.3. Hydrogen Bonding and Miscibility Behavior of Polymer/POSS Nanocomposites

6.3.1. Hydrogen Bonding Interactions Between Polymers and POSS

The miscibility and specific interactions of polymer blends attract great attention in polymer science because of their significant potential applicability in industry. Most inorganic silicas or creamers are immiscible in most organic polymer systems because of poor specific interactions within these organic/inorganic hybrids and the negligibly small combined entropy contribution to the free energy of mixing. Specific intermolecular interactions are generally required to enhance the miscibility of polymers and inorganic particles.

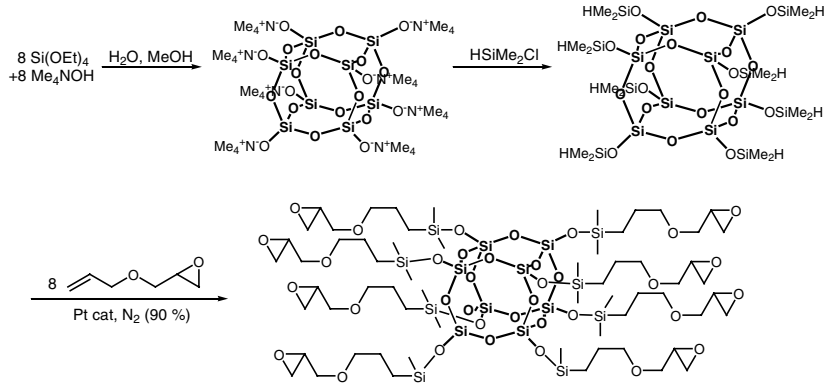

Figure 6.5 An example of multifunctional POSS synthesis.

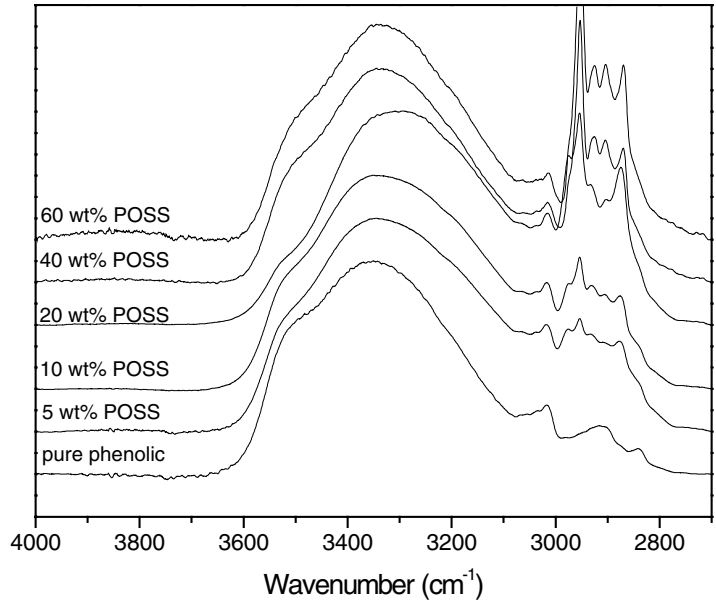

Figure 6.6 FT-IR spectra of phenolic/POSS hybrid with various POSS contents.

To improve properties and miscibility of hybrid materials, it is usually necessary to ensure that favorable specific interactions exist between these components, such as hydrogen bonding, dipole–dipole interactions, or acid/base complexation [29]. Determining the types and strengths of the interactions between POSS derivatives and polymers is an important challenge. For convenience, Chang et al. blended phenolic resin with a POSS derivative to investigate the miscibility, specific interactions, and microstructural behavior [30]. Figure 6.6 displays IR spectra (2700–4000 cm^{-1}) of pure phenolic and various phenolic/POSS hybrids measured at room temperature [30].

The spectrum of the pure phenolic polymer contains two OH components: a very broad band centered at 3350 cm^{-1} that is attributed to the wide distribution of the

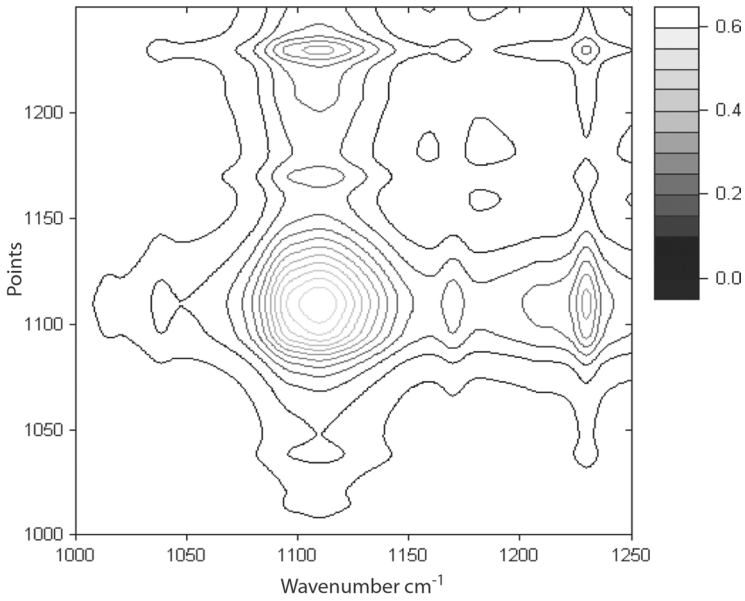

Figure 6.7 The synchronous 2D correlation map at 1000–1250 cm^{-1} region.

hydrogen-bonded OH groups and a relatively narrow band at 3525 cm^{-1} corresponding to free OH groups. Two trends are observed for the OH stretching bands in the IR spectra of the phenolic/POSS hybrids: the broad hydrogen-bonded OH band of phenolic shifts to lower wavenumber upon increasing the POSS content, approaching a minimum at 3280 cm^{-1} for the hybrid containing 20 wt% POSS (Figure 6.6 (d)) [30].

This change arises from the switch of intramolecular hydroxyl–hydroxyl to intermolecular hydroxyl–siloxane interactions, i.e., hydrogen bonding between the OH groups of phenolic, and the siloxane groups of POSS. Generalized 2D IR correlation spectroscopy was used to explore the nature of the hydrogen bonding sites in the phenolic/POSS hybrid. This tool can be used to study the mechanism of interpolymer miscibility through the formation of hydrogen bonds, both qualitatively and quantitatively. Using this novel method, spectral fluctuations can be treated as a function of time, temperature, pressure, or composition to investigate the specific interactions occurring between polymer chains. 2D IR correlation spectroscopy can identify different intra- and intermolecular interactions through selected bands from a 1D vibration spectrum [31]. Figure 6.7 presents the synchronous 2D correlation maps of set A in the range from 1250 to 1000 cm^{-1}. The absorption bands of the POSS derivative at 1100 and 1230 cm^{-1} correspond to siloxane Si–O–Si and Si–C stretching vibrations, respectively. The 1223 cm^{-1} peak is due to the phenyl–OH stretching vibration of the phenolic. There are two positive cross-peaks shown in Figure 6.7, indicating hydrogen bonding interactions between the siloxane group of the POSS derivative (1100 cm^{-1}) and the phenyl–OH group (1223 cm^{-1}) of the phenolic.

6.3.2. Miscibility Between Polymers and POSS Derivatives

The most important feature of a miscible polymer blend is that interassociation is stronger than self-association. Conversely, if the self-association is stronger than the interassociation, the blend tends to be immiscible or only partially miscible. According to the

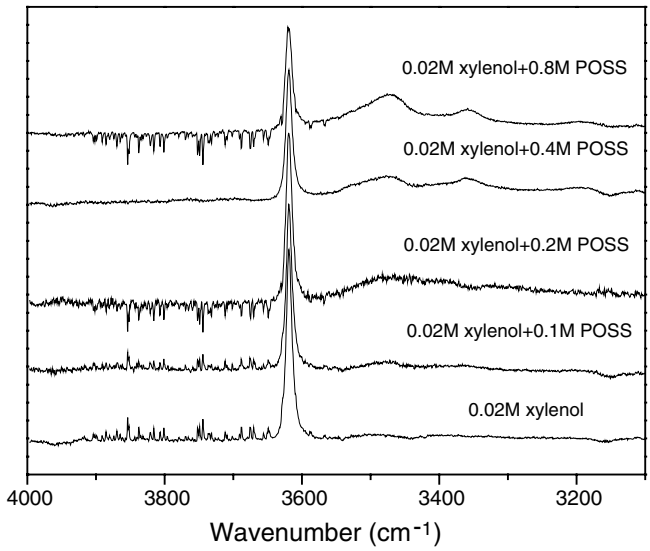

Figure 6.8 FT-IR spectra of 2,4-dimethylphenol with various POSS concentrations.

Painter–Coleman association model (PCAM) [29], the interassociation equilibrium constant between a noncarbonyl group component and a hydrogen bond donating component can be calculated using the classical Coggeshall and Saier (C&S) method. Figure 6.8 displays the OH group absorption of 2,4-dimethylphenol (a model compound for phenolic) in cyclohexane solutions containing various concentrations of POSS; the intensity of the free OH absorption at 3620 cm^{-1} decreases with increasing POSS content. The absolute intensity of the free OH group at 3620 cm^{-1} is assumed to be an indication of the content of free OH groups in the mixture [30]. Figure 6.8 indicates that the frequency of the associated OH band shifts from free OH group at 3620 to 3490 cm^{-1} as a result of interassociation hydrogen bonding between 2,4-dimethylphenol and POSS [30]. The interassociation equilibrium constant, K_A, yielded through this procedure is 38.6, based on the classic C&S method [32], whereas the self-association equilibrium constant for the phenolic is 52.3 [33]. Clearly, the interassociation equilibrium constant from the phenolic/POSS is relatively lower compared with the self-association equilibrium constant of pure phenolic, indicating that the phenolic/POSS hybrid is partially miscible or immiscible because of its relatively poor intermolecular association [34].

For this reason, functionalization of POSS derivatives possessing pendent hydrogen bond acceptor groups is expected to improve the miscibility with phenolic resin. Functionalization of $Q_8M_8^H$ can be achieved through hydrosilylation of its Si–H groups with acetoxystyrene [34] in the presence of a Pt catalyst to form AS-POSS (Figure 6.9).

Figure 6.10 presents scaled IR spectra, recorded at room temperature, of pure phenolic and various phenolic/AS–POSS nanocomposites. Figure 6.10(a) indicates clearly that the intensity of the free OH absorption (3525 cm^{-1}) decreases gradually as the AS-POSS content of the blend is increased from 5 to 90 wt%. The band for the hydrogen-bonded OH units in the phenolic tends to shift to higher frequency (toward 3465 cm^{-1}) upon increasing the AS-POSS content. This change is due to the switch from hydroxyl–hydroxyl interactions to the formation of hydroxyl–carbonyl and/or hydroxyl–siloxane hydrogen

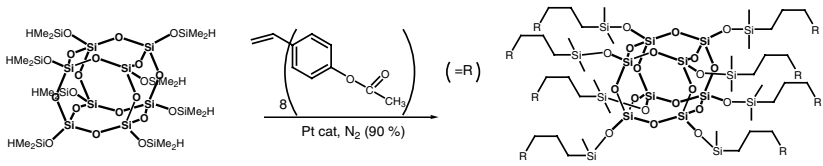

Figure 6.9 Chemical structures of AS-POSS.

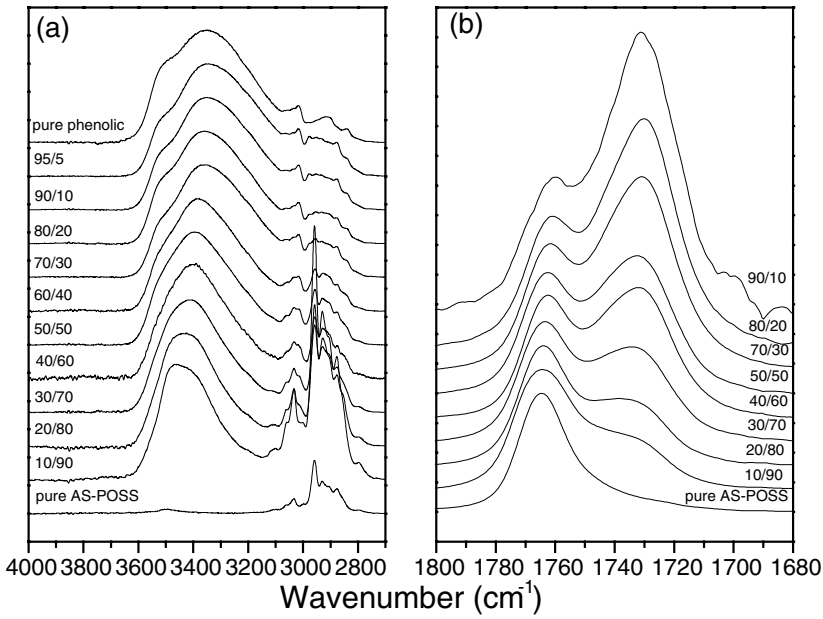

Figure 6.10 IR spectra for phenolic/AS-POSS blends: (a) hydroxyl and (b) carbonyl.

bonds. Figure 6.10(b) displays IR spectra (1680–1820 cm^{-1}) measured at room temperature for various phenolic/AS-POSS blend composites. The C=O stretching frequency is split into two bands at 1763 and 1735 cm^{-1} corresponding to the free and hydrogen-bonded C=O groups, respectively. These bands are readily decomposed into two Gaussian peaks corresponding to areas of the hydrogen-bonded C=O (1735 cm^{-1}) and the free C=O (1763 cm^{-1}) peaks [35].

According to the PCAM, the interassociation equilibrium constant between a noncarbonyl group component and a hydrogen bond donating component can be calculated using the classical C&S method. To recheck the interassociation equilibrium constant between the phenolic OH groups and the POSS siloxane groups, the value of K_A can be determined indirectly from a least-squares fitting procedure of the experimental fraction of hydrogen-bonded C=O groups of AS-POSS in this binary blend. Figure 6.11 indicates that the experimental values are generally lower than the predicted values when using the value of K_A of 64.6 obtained from the phenolic/PAS blends [36]. This result also indicates that the OH groups of phenolic not only interact with the C=O groups of the acetoxystyrene units but also with the siloxane groups of the POSS core, which is consistent with the results

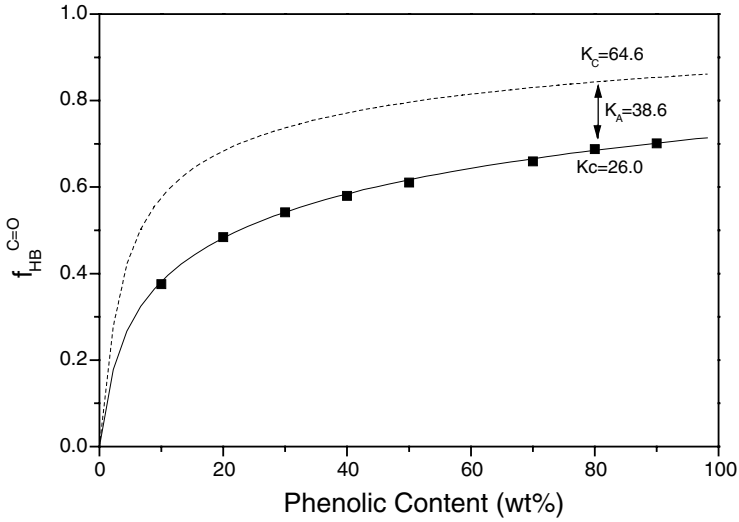

Figure 6.11 Fraction of hydrogen-bonded carbonyl groups versus phenolic contents.

reported from a previous study. To calculate the values of the interassociation constants K_A, a least-squares method was employed as described previously [36], which resulted in an interassociation equilibrium constant of 26.0 for the phenolic/AS-POSS blend. The value of K_A obtained from the phenolic/PAS blend was 64.6, implying that the value of K_A between the OH group of phenolic and the siloxane group of POSS is equal to 38.6 (i.e., $64.6 - 26.0 = 38.6$), which is exactly consistent with the value reported previously based on classical C&S methodology [32]. Therefore, there is a good correlation between these two different methods when determining the values of the interassociation equilibrium constants for hydroxyl–siloxane interactions. In addition, the trend of the glass transition temperature (T_g) of the phenolic/AS-POSS blend (q = 25) is greater than that of the phenolic/PAS blend ($q = -245$) system based on the Kwei equation [37].

This behavior may arise from two phenomena: (i) the star-shaped acetoxystyrene-POSS presents a larger fraction of hydrogen-bonded C=O groups than does the linear PAS, which is similar to the findings made in a previous study of a phenolic/poly(methyl methacrylate) blend system [38]; (ii) the siloxane groups of the POSS core can also form hydrogen bonds with the OH groups of the phenolic. Therefore, the presence of POSS moieties effectively increases the values of T_g of the resultant organic/inorganic polymer nanocomposites.

The low molecular weight of POSS derivative is unable to effectively increase the glass transition temperature in the phenolic/AS-POSS blend system. As a result, Lin et al. synthesized a new POSS derivative containing eight phenol groups and then copolymerized it with phenol and formaldehyde to form novolac-type phenolic/POSS nanocomposites through covalent bonding, which exhibits high thermal stabilities and low surface energies (Figure 6.12) [39].

Figure 6.13 displays conventional second-run DSC and TGA thermograms of phenolic/OP–POSS nanocomposites at various weight ratios [39]. Each of these hybrids possesses essentially a single value of T_g, suggesting that these hybrids exhibit a single phase. The glass transition temperatures of these nanocomposites are significantly enhanced after incorporation of POSS units; however, fractions of incompletely reacted

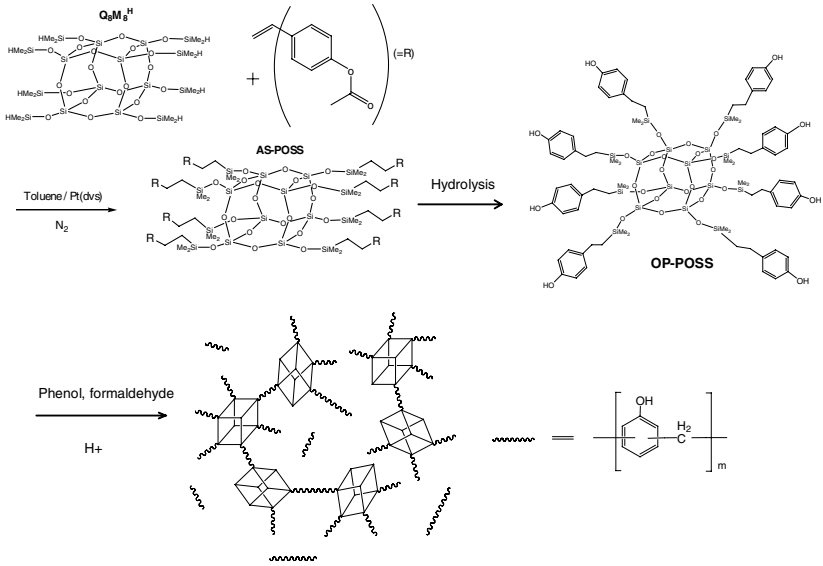

Figure 6.12 Synthesis procedure of phenolic/OP–POSS nanocomposites.

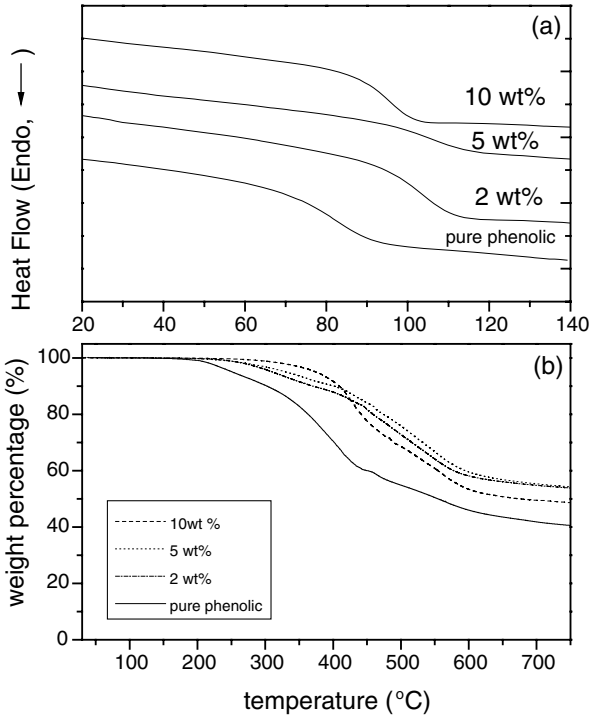

Figure 6.13 Thermal analyses of phenolic/OP–POSS nanocomposites containing different OP–POSS contents: (a) DSC and (b) TGA.

functional groups are still remained on the POSS and phenolic components. The enhanced glass transition temperature is resulted from the restricted motion of the polymer chains caused by the physical crosslinkage through hydrogen bonding interactions from these evenly distributed POSS units within the phenolic matrix. Figure 6.13(b) shows thermal degradation of neat phenolic resin and the POSS-containing nanocomposites [39].

The char yield increases upon increasing the POSS content except the sample incorporating 10 wt% POSS, providing further evidence that some lower molecular weight species are still present in the phenolic/octaphenol-POSS 10 wt% sample. The value of T_d increases significantly upon increasing the POSS content, the phenolic/OP–POSS 10 wt% sample exhibits a value of T_d 123°C higher than that of the pure phenolic resin. This phenomenon can be explained in terms of the nano-reinforcement effect of incorporating POSS moieties into polymeric matrixes. The nanoscale dispersion of POSS moieties within the matrix and their covalent and hydrogen bonds to the phenolic resin are responsible for enhancing the initial decomposition temperature [39].

6.4. POSS-Containing Polymers and Copolymers

POSS feedstocks, which have been functionalized with various reactive organic groups, can be incorporated into virtually any existing polymer system through either grafting or copolymerization. POSS homopolymers can also be synthesized. The incorporation of the POSS nanocluster cages into polymeric materials can result in dramatic improvements in polymer properties, including temperature and oxidation resistance, surface hardening, and reduction in flammability. Therefore, research in POSS-related polymers and copolymers has accelerated recently. Some representative systems are discussed below.

6.4.1. Polyolefin/POSS and Norbornyl/POSS Copolymers

A number of interesting design strategies for the preparation of polyolefin/POSS hybrid materials have evolved over the past decade. Hsiao et al. [40] used DSC to investigate a series of iPP melt-blended with nanostructured POSS molecules to study the quiescent melt crystallization behavior, and shear-induced crystallization behavior. Tabuani and coworkers [41, 42] reported the influence of the POSS substituent groups on the morphological and thermal characteristics of melt-blended PP/POSS composites. Furthermore, Coughlin et al. and Mather et al. reported polyolefin copolymers containing norbornyl-POSS macromonome [43–45]. Polyolefin-POSS copolymers incorporating a norbornylene-POSS macromonomer have been prepared using a metallocene/methyl aluminoxane (MAO) cocatalyst system (Figure 6.14) [43].

6.4.2. Polystyrene/POSS Nanocomposites

Haddad synthesized and characterized (Figure 6.15) a series of linear thermoplastic hybrid materials containing an organic polystyrene backbone and large inorganic silsesquioxane groups pendent to the polymer backbone [46]. The pendent inorganic groups drastically modify the thermal properties of the polystyrene, and the interchain and/or intrachain POSS–POSS interactions affected the solubility and thermal properties [46].

Couglin et al. [47] developed a synthetic route for preparing syndiotactic PS (sPS)–POSS copolymers (Figure 6.16). Copolymerizations of styrene and POSS afforded a novel nanocomposite of sPS and POSS. The rate of copolymerizations was much slower than

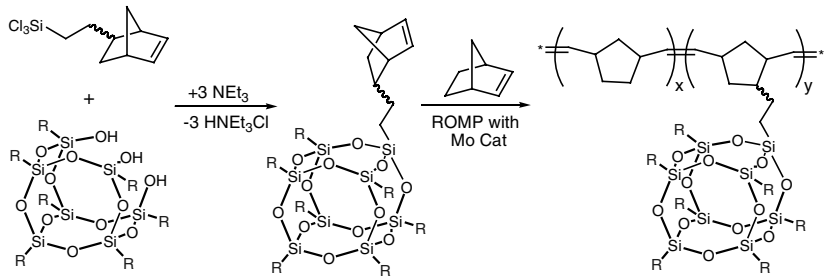

Figure 6.14 Copolymerization of norbornylene-POSS and norbornene

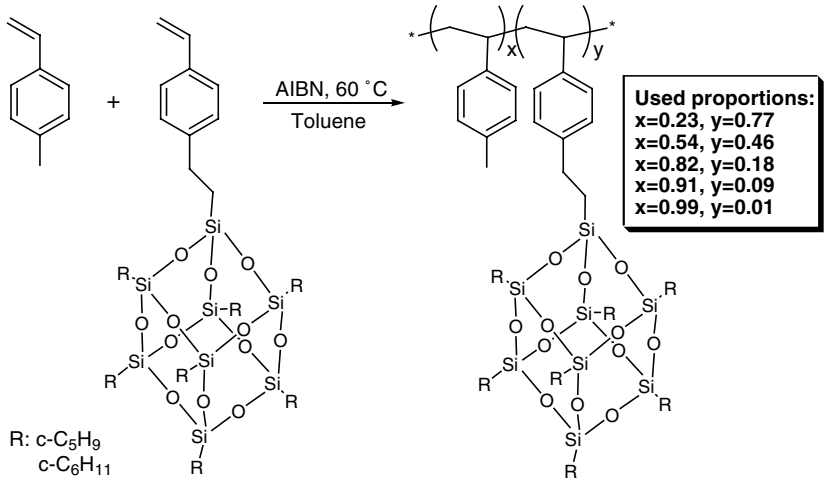

Figure 6.15 POSS styryl macromer synthesis and polymerization.

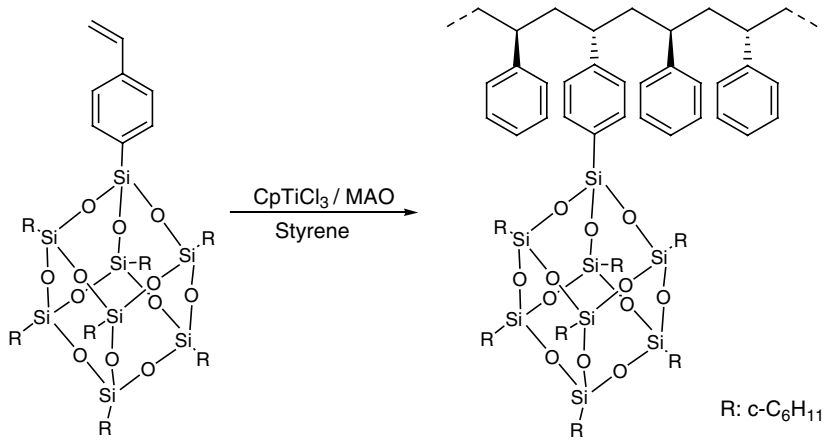

Figure 6.16 Copolymerization of styrene and POSS-styryl.

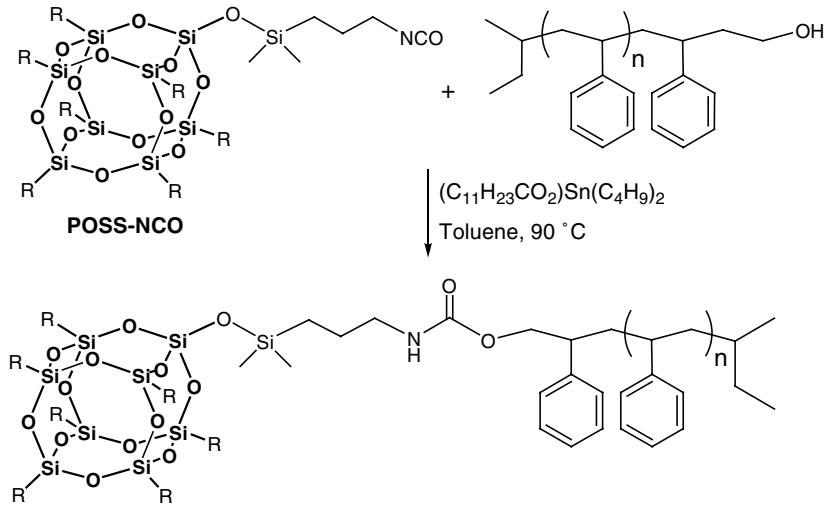

Figure 6.17 Synthesis of hemi-telechelic POSS–polystyrene hybrid.

that of radical polymerization, presumably because of the coordination polymerization mechanism. TGA traces of the sPS–POSS copolymers under both nitrogen and air revealed their improved thermal stability, i.e., higher degradation temperatures and char yields [47].

Couglin et al. also reported a synthetic protocol for preparing well-defined POSS–polystyrene hemi-telechelic hybrids (Figure 6.17) [48]. These model systems provide the opportunity to experimentally probe the ordering or aggregation behavior of inorganic nanoparticles within polymeric matrices.

Chang et al. synthesized and characterized a series of hybrid poly (acetoxylstyrene-*co*-isobutylstyryl-POSS) (PAS–POSS) systems [49, 50]. The presence of the POSS moiety effectively increases the glass transition temperatures of the resultant organic/inorganic hybrid polymers at relatively high POSS contents. Furthermore, a series of poly(hydroxystyrene-*co*-vinylpyrrolidone-*co*-isobutylstyryl-POSS) hybrid polymers incorporating various POSS contents were prepared through free radical copolymerization of acetoxystyrene, vinylpyrrolidone, and POSS, followed by selective removal of the acetyl protecting group [51, 52]. The value of T_g of the PHS–PVP–POSS hybrids increases substantially upon incorporating the POSS moiety (Figure 6.18). The presence of the physically crosslinked POSS through hydrogen bonding in these hybrid polymers tends to restrict the polymer chain motion, and results in higher T_g.

Figure 6.19 displays the C=O stretching region (1620–1720 cm^{-1}) of FTIR spectra recorded at room temperature of different concentrations of ethylpyrrolidone (EPr, a model compound for PVP) in cyclohexane, PAS-*co*-PVP-*co*-POSS2.2, PAS-*co*-PVP, pure PVP, PVPh/PVP blend, PVPh-*co*-PVP, PVPh-*co*-PVP-*co*-POSS0.8, PVPh-*co*-PVP-*co*-POSS2.2, and PVPh-*co*-PVP-*co*-POSS3.2 copolymers [51, 52]. The C=O band of the EPr/cyclohexane solution is broaden and shifted to lower wavenumber upon increasing the EPr concentration because of higher probability of forming pyrrolidone/pyrrolidone interactions. These results confirm that the wavenumber and half-width are both dependent upon the specific and dipole interactions between molecules or polymer chains. In addition, the signal for the pure PVP homopolymer appeared at lower wavenumber and gives a

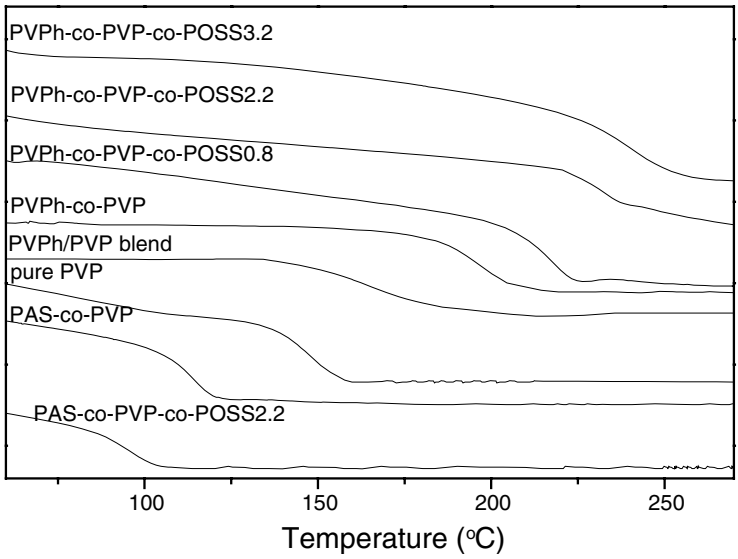

Figure 6.18 DSC thermograms of PAS-*co*-PVP-*co*-POSS, PAS-*co*-PVP, pure PVP, PVPh/PVP blend, PVPh-*co*-PVP, and with different POSS contents of PVPh-*co*-PVP-*co*-POSS.

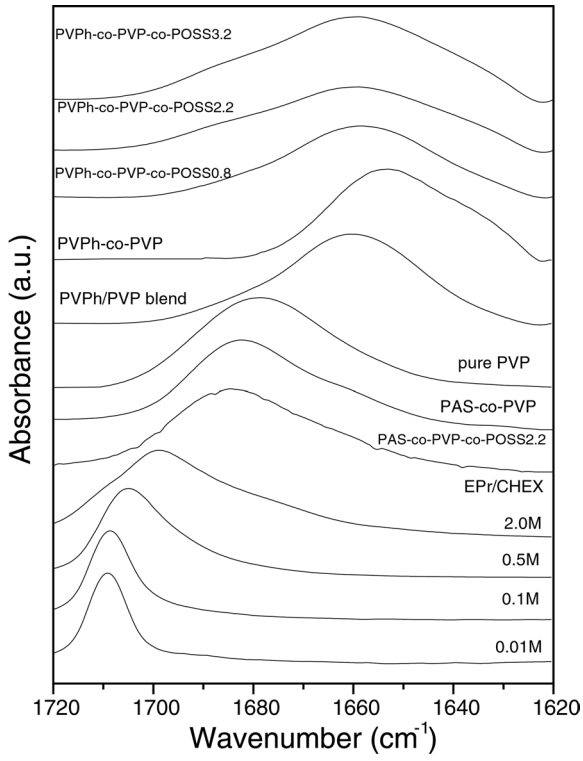

Figure 6.19 FTIR spectra for various EPr concentrations in cyclohexane, PAS-*co*-PVP-*co*-POSS, PAS-*co*-PVP, pure PVP, PVPh/PVP blend, PVPh-*co*-PVP, and with different POSS contents of PVPh-*co*-PVP-*co*-POSS.

broader half-width relative to that of EPr in cyclohexane because no inert diluent (nonpolar) group is present in the pure PVP homopolymer. Therefore, the probability of dipole–dipole interactions of the PVP is expected to be greater than that in the EPr/cyclohexane system. Upon incorporation of acetoxystyrene monomers into the PVP chain, the half-width of the PVP C=O band at 1680 cm^{-1} decreases and shifts to higher wavenumber (1682 cm^{-1}). The value of T_g of PAS-*co*-PVP decreases significantly (26°C) as a result of the lower degree of dipole–dipole interactions of the pyrrolidone moieties in the polymer chain. The C=O band of the PAS-*co*-PVP at 1682 cm^{-1} shifts slightly higher (to 1683 cm^{-1}) upon incorporation of the POSS moiety into the PAS-*co*-PVP copolymer chain. It appears that the incorporation of the inert diluent group (POSS) into the polymer chain decreases the strength of its original dipole–dipole interactions [51, 52].

For this reason, the T_g of PAS-*co*-PVP-*co*-POSS2.2 also decreases significantly (24°C) relative to that of the PAS-*co*-PVP copolymer. This result provides evidence for why most POSS hybrid polymer systems possess lower T_g, relative to those of the original polymer matrices, at lower POSS contents. Figure 6.20 displays all the shifts and interactions of the characteristic vibration bands [51, 52].

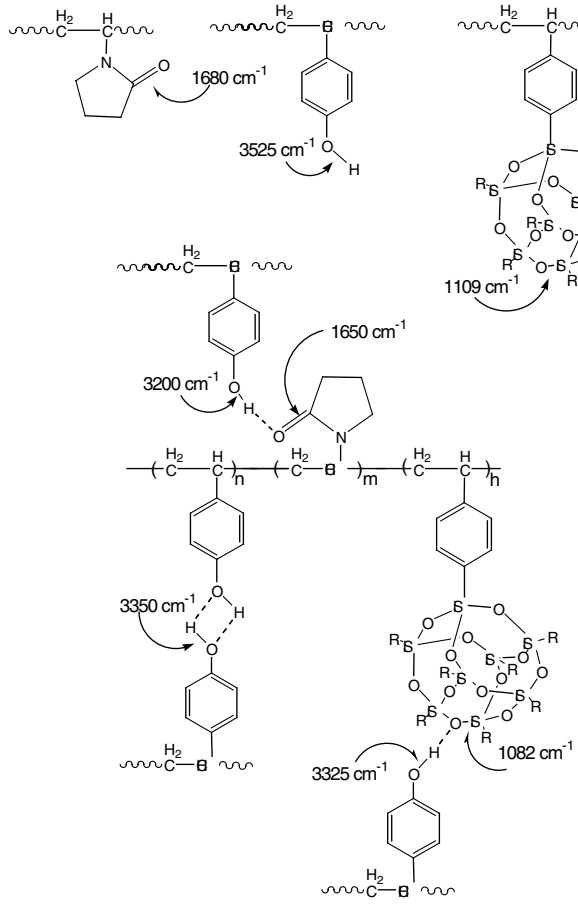

Figure 6.20 Interaction of POSS and PVPh.

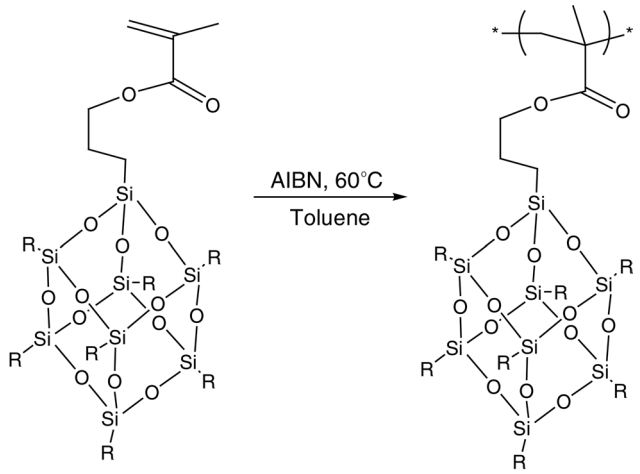

Figure 6.21 Synthesis of PMMA–POSS nanocomposites.

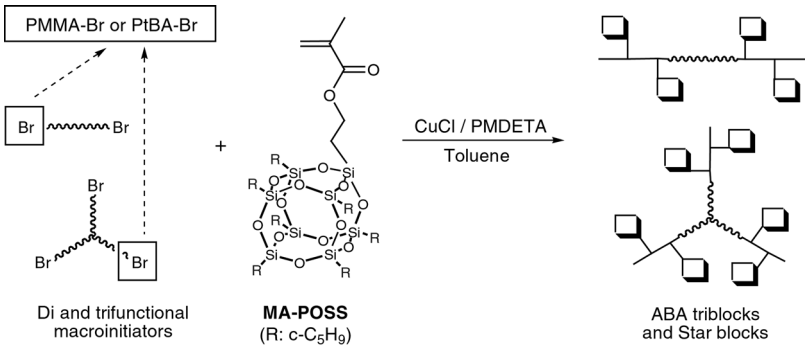

Figure 6.22 Synthesis of triblock and star-block copolymers.

6.4.3. Poly(methacrylate)/POSS Copolymers

Methacrylate-substituted POSS macromers can be prepared containing one polymerizable functional group (Figure 6.21) [53–60]. The resulting materials are generally transparent brittle plastics, i.e., the incorporation of the POSS group into linear polymers tends to prevent or reduce the segmental segregation or mobility.

Pyun and Matyjaszewski used atom transfer radical polymerization (ATRP) to synthesize an MA-POSS homopolymer and block copolymers from a cyclopentyl-substituted POSS monomer [60, 61]. They employed ATRP to prepare the block copolymer of MA-POSS with *n*-butyl acrylate; 4-(methylphenyl) 2-bromoisobutyrate as the initiator and CuCl/PMDETA as the catalyst (Figure 6.22) [60, 61]. Triblock copolymers were prepared from a difunctional (both ends) bromine-terminated poly(*n*-butyl acrylate) macroinitiator ($M_{n,\mathrm{NMR}} = 7780$) and MA-POSS. In the syntheses of the triblock copolymers, the macroinitiator was prepared through ATRP of *n*-BA using dimethyl-2,6-dibromoheptanedioate as the difunctional initiator. Synthesis of P(MA-POSS)-*b*-PBA-*b*-P(MA-POSS) triblock and PMA-*b*-P(MA-POSS) star-block copolymers were carried out

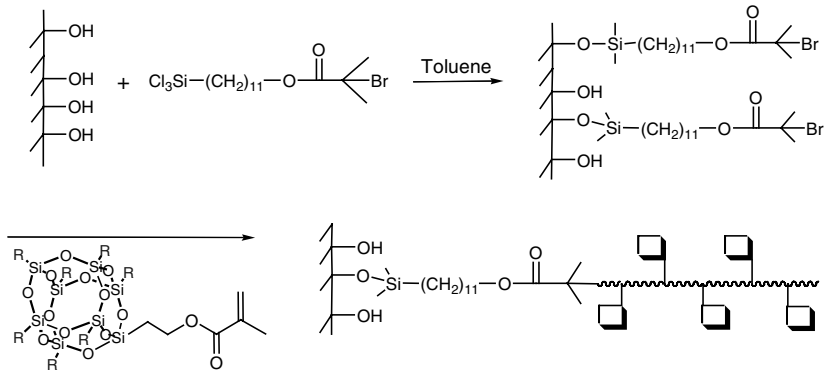

Figure 6.23 Surface-initiated ATRP of POSS-MA.

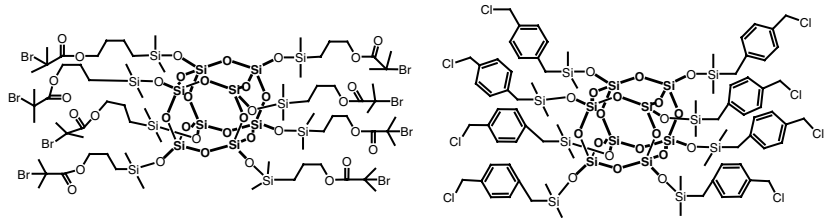

Figure 6.24 ATRP initiators of octafunctional silsesquioxane cube.

by chain extension of the difunctional bromine-terminated *n*-butyl acrylate macroinitiator using MA-POSS monomer. A star-block copolymer of methyl methacrylate and MA-POSS were also prepared through ATRP of methyl methacrylate using a trifunctional initiator. The polydispersity (M_w/M_n) of this star block copolymer was 1.30 [60, 61].

TEM characterization of the triblock copolymer thin film P(MA-POSS)$_{10}$-b-PBA$_{201}$-b-P(MA-POSS)$_{10}$ revealed the formation of PBA cylinders in a P(MA-POSS) matrix. Chen et al. reported the polymerization of an isobutyl-substituted MA-POSS monomer from a self-assembled monolayer (SAM) of ATRP initiators covalently immobilized on flat silicon wafers (Figure 6.23) [62]. This method is a simple and effective approach toward preparing well-defined POSS-containing polymer films from flat surfaces [62].

AQ1: Please provide the missing reference number in the sentence 'A further investigation [ref]…'

Laine et al. synthesized a star poly(methyl methacrylate) from an octafunctional silsesquioxane cube using the "core-first" method and ATRP (Figure 6.24) [63].

Fukuda and co-workers used an incompletely condensed POSS possessing a highly reactive trisodium silanolate group for the synthesis of several initiators for ATRP to obtain tadpole-shaped polymeric hybrids with a POSS unit at the end of the polymer chain (Figure 6.25) [64, 65].

Recently, Chang et al. reported polymer hybrids having controllable molecular weights and a chain-end-tethered POSS moiety synthesized through ATRP (Figure 6.26) [66].

Blending both PMMA–POSS and PMMA with phenolic resin revealed that the POSS terminus affected the thermal properties, miscibility behavior, and hydrogen bonding interactions [66]. A further investigation [ref] of the specific interassociation interactions between the terminal siloxane units of the POSS moieties and the OH groups

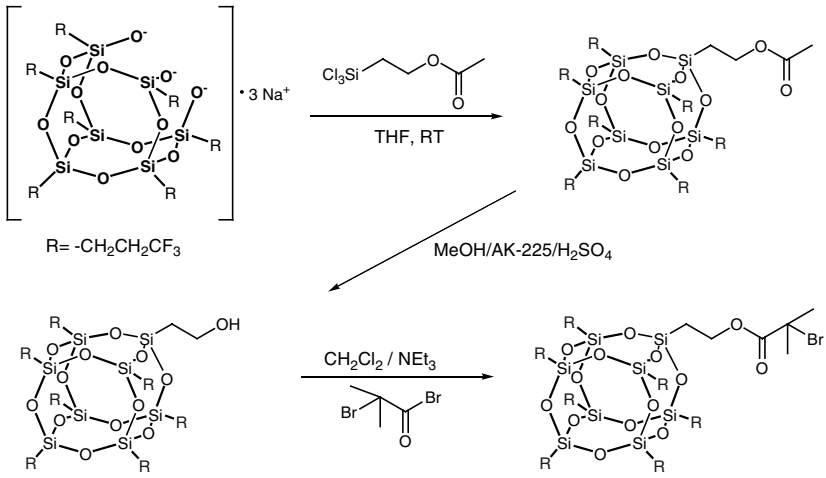

Figure 6.25 Synthesis of fluorinated POSS-Holding Initiator 7F-T8-BIB.

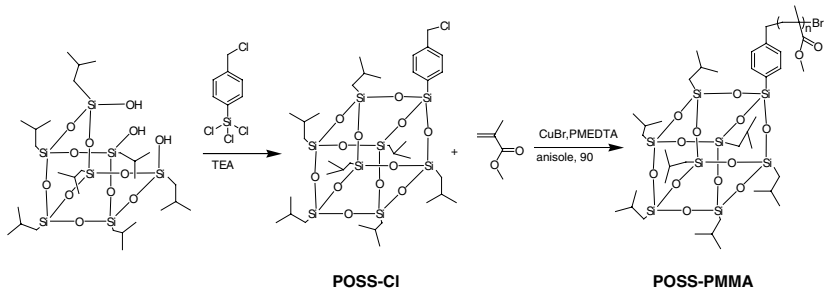

Figure 6.26 Synthetic route to prepare PMMA–POSS and PMMA polymers.

of the phenolic revealed an interesting "screening effect" in these phenolic and low-molecular-weight PMMA–POSS blends (less than PMMA entanglement), as indicated in Figure 6.27 [66].

6.4.4. Poly(ethylene oxide)/POSS Nanocomposites

Poly(ethylene oxide) (PEO) is an important polymer electrolyte in lithium ion batteries because of its ability to solvate lithium ions. Nevertheless, it is a semicrystalline polymer and ionic conduction occurs mostly in the amorphous phase; the room temperature (RT) ionic conductivity of PEO is low due to its crystallization. The ion mobility increases with greater free volume upon increasing the number of chain ends; therefore, higher conductivity is expected for low-molar-mass or highly branched PEO polymers compared with linear, high-molar-mass PEO. Thus, one approach toward increasing the RT conductivity of PEO-based polymer electrolytes is the attachment of short-chain PEO oligomers as side chains to form "comb-shaped" or "hairy rod"-like polymeric structures, or as "arms" from inorganic scaffolds. Wunder et al. [67] grafted oligomeric PEO chains onto $Q_8M_8^H$ to produce the PEO functionalized silsesquioxanes as displayed in Figure 6.28.

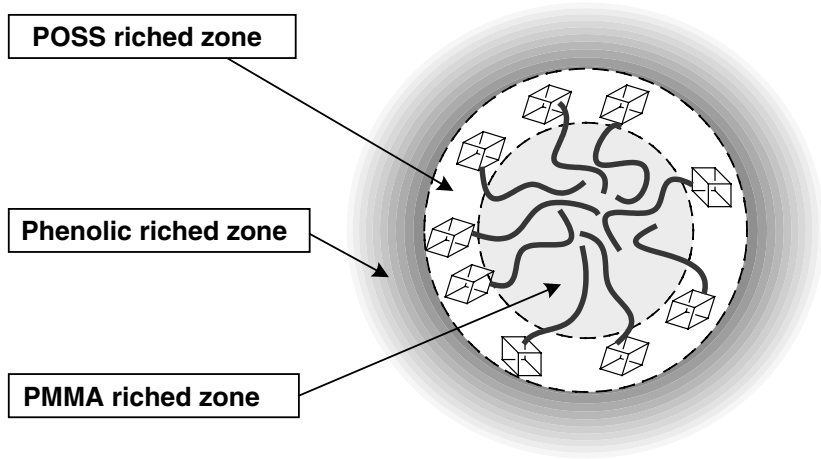

Figure 6.27 Proposed screening effect microstructure in phenolic/PMMA–POSS blends.

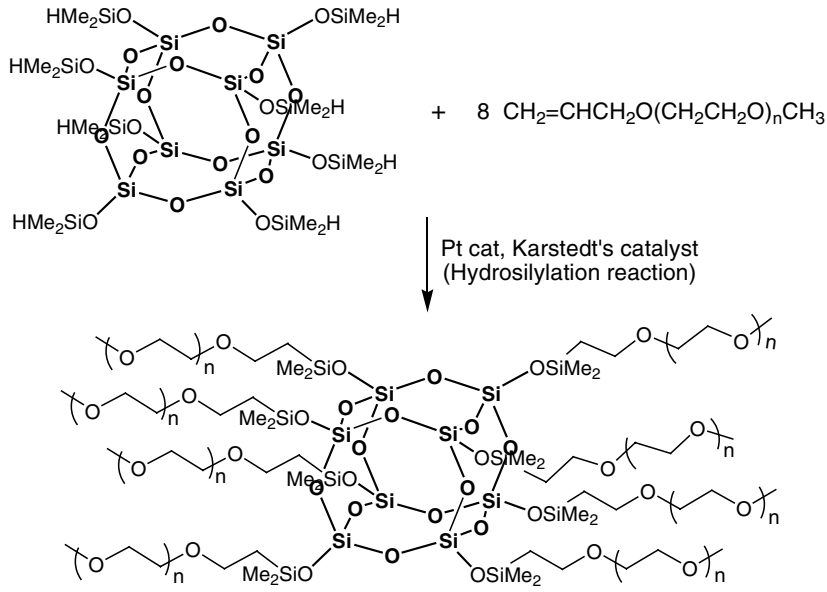

Figure 6.28 Reaction scheme to prepare PEO-octafunctionalized silsesquioxanes.

A strong self-supporting film prepared from 10% methyl cellulose and 90% Q_8M_8PEO (n = 8)/$LiClO_4$ resulted in RT conductivity of 10^{-5} S/cm [67].

In addition, well-defined amphiphilic telechelics incorporating POSS have been synthesized through direct urethane linkage between the OH end groups of a poly(ethylene glycol) (PEG) homopolymer and the monoisocyanate groups of a POSS macromer, as indicated in Figure 6.29 [68].

They found that the synthesized amphiphilic telechelics exhibited a relatively narrow and unimodal molecular weight distribution (M_w/lM_n < 1.1) and had close to 2.0 end

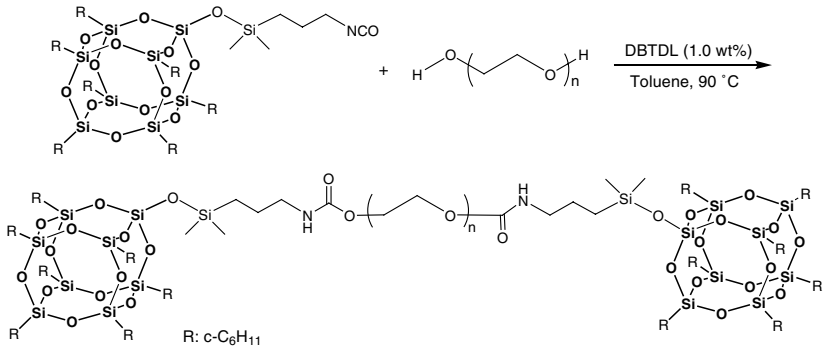

Figure 6.29 Reaction scheme of the amphiphilic telechelics incorporating POSS.

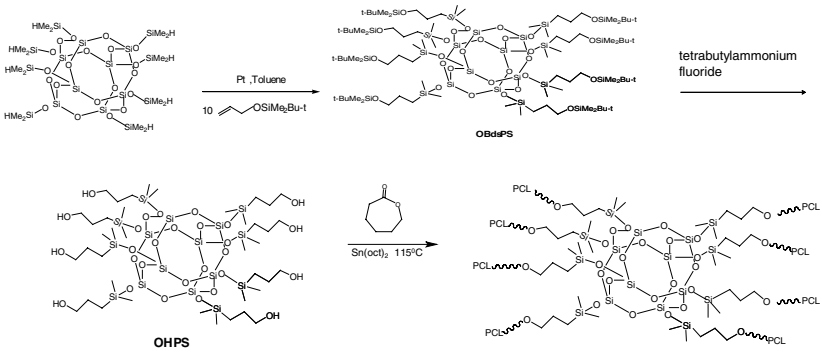

Figure 6.30 Synthesis of OHPS-cored eight-arm PCL star polymers.

groups per PEG chain [68]. The crystallinity of the PEO segments in the amphiphilic telechelics decreased dramatically when the POSS content in the amphiphilic telechelic reached 40.7%, and became amorphous at values beyond ca. 50%. As a result, they obtained several amphiphilic telechelics with a range of thermal and morphological properties through controlling the ratio of the hydrophilic PEG homopolymer and the hydrophobic and bulky POSS macromers [68].

6.4.5. PCL/POSS Nanocomposites

Chang et al. synthesized a series of the organic/inorganic hybrid star PCLs through coordinated ring-opening polymerization of ε-caprolactone using POSS as the initiator (Figure 6.30) [69].

Similar to the linear PCL analogues reported previously, this star PCL formed inclusion complexes (ICs) with α- and γ-CD, but not with β-CD [69]. The stoichiometries of all the ICs with α- and γ-CD were greater than those of the corresponding CD/linear PCL ICs because of steric hindrance around the bulky POSS core and some g of the gε-caprolactone units near the core were unable to form ICs. Zheng et al. [70] reported another approach for the preparation of octa(3-hydroxypropyl) POSS; they used an octafunctional initiator for the synthesis of eight-armed star-shaped PCLs. Organic/inorganic star PCLs possessing

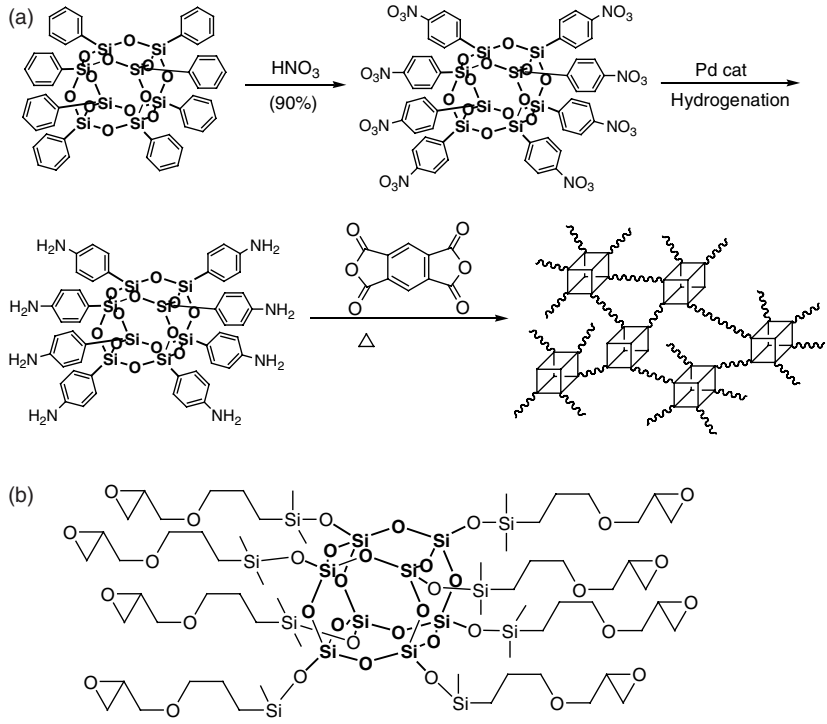

Figure 6.31 (a) Laine's (b) Lee's.

various degrees of polymerization were synthesized via ring-opening polymerization catalyzed by stannous(II) octanoate [$Sn(Oct)_2$] [70].

6.4.6. Polyimide/POSS Nanocomposites

Polyimides (PIs) are widely used in microelectronics industries because of their outstanding characteristics, such as excellent tensile strength and modulus, good thermal stability and dielectric properties, and high resistance to organic solvents. There are two common routes for incorporating POSS units into a PI matrix. One method of achieving PI–POSS nanocomposites is to use a POSS derivative possessing eight functional groups (e.g., epoxy or amino groups) to serve as a crosslinking agent. Laine and co-workers described [71, 72] the nitration of octa-phenyl POSS, which was first reported in 1961 by Olsson [72], and subsequent production of octakis(aminophenyl)–POSS through Pd/C-catalyzed hydrogenation (Figure 6.31(a)).

Furthermore, the octa-amino POSS was employed in conjunction with dianhydrides to prepare extremely thermally resistant crosslinked PI networks [71, 72]. This amino-POSS derivative can be reacted with maleic anhydride to obtain the octa-*N*-phenylmaleimide [73], which can also serve as a crosslinking agent in maleimide polymer chemistry. He et al. [74] and Chang et al. [75] demonstrated that the PI prepolymer, polyamic acid (PAA), can react with octakis(glycidyldimethylsiloxy)-octasilsesquioxane (Figure 6.31(b)).

Using these approaches, the dielectric constants of the PI nanocomposites can be reduced, and their thermal properties modified, upon increasing the POSS content.

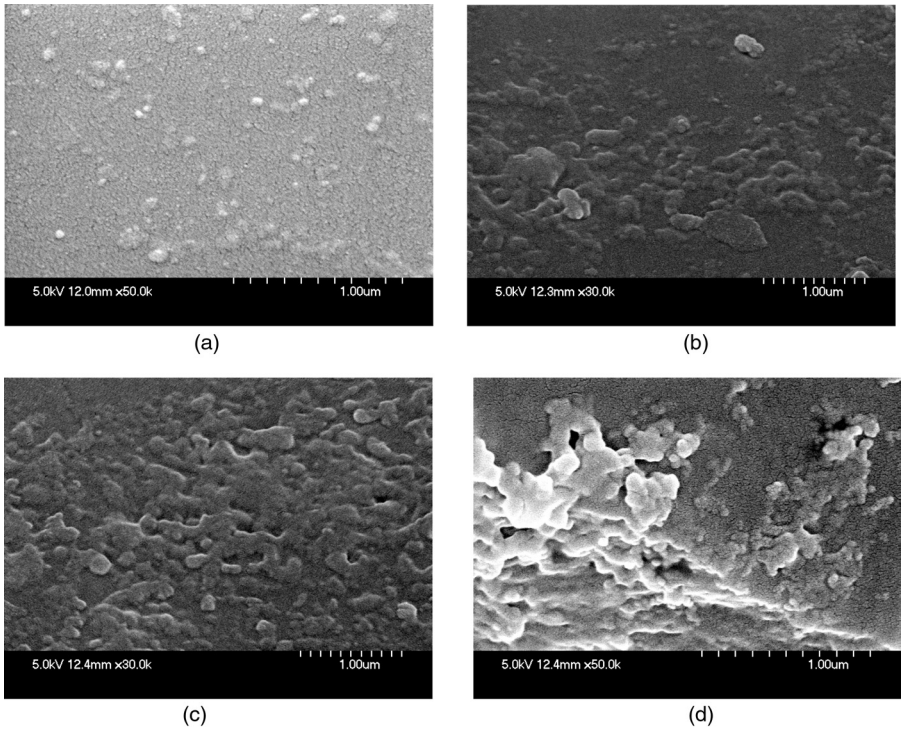

Figure 6.32 SEM cross-section analysis of PI–POSS hybrid materials (a) PI-3P, (b) PI-7P, (c) PI-10P. (d) Fractured cross-section surface of the PI-10P.

Figures 6.32(a)–(d) display cross-sectional SEM images of various morphologies obtained at various epoxy-POSS contents. In this study, excess diamine (ODA) was reacted initially with BTDA and then the terminal amino groups of the polyamic acid were reacted with epoxy-POSS. By varying the equivalent ratio of the ODA, polyamic acids of various molecular weights and nanocomposites possessing various morphologies were obtained. The reduction in the dielectric constant of the PI–POSS hybrids can be explained in terms of the nanovoid volume of the POSS cores and the free volume increase resulting from the presence of the rigid, large POSS units inducing a loose PI network (Figure 6.32(d)) [75].

Wei et al. [76–78] reported the grafting reaction of a novel POSS derivative as an approach toward PI-tethered POSS nanocomposites possessing well-defined architectures (Figure 6.33). These types of PI-tethered POSS nanocomposites have both lower and tunable dielectric constants, with the lowest value of 2.3, and controllable mechanical properties, relative to those of the pure PI. The tethered POSS molecules in the amorphous PI retain a nanoporous crystal structure, but form an additional ordered architecture as a result of microphase separation. Using this approach, the dielectric constant of the film can be tuned by modifying the amount of POSS added [76–78].

6.4.7. Epoxy/POSS Nanocomposites

Monofunctional and multifunctional POSS–epoxies have been incorporated into the backbones of epoxy resins to improve their thermal properties [79–84]. The multifunctional

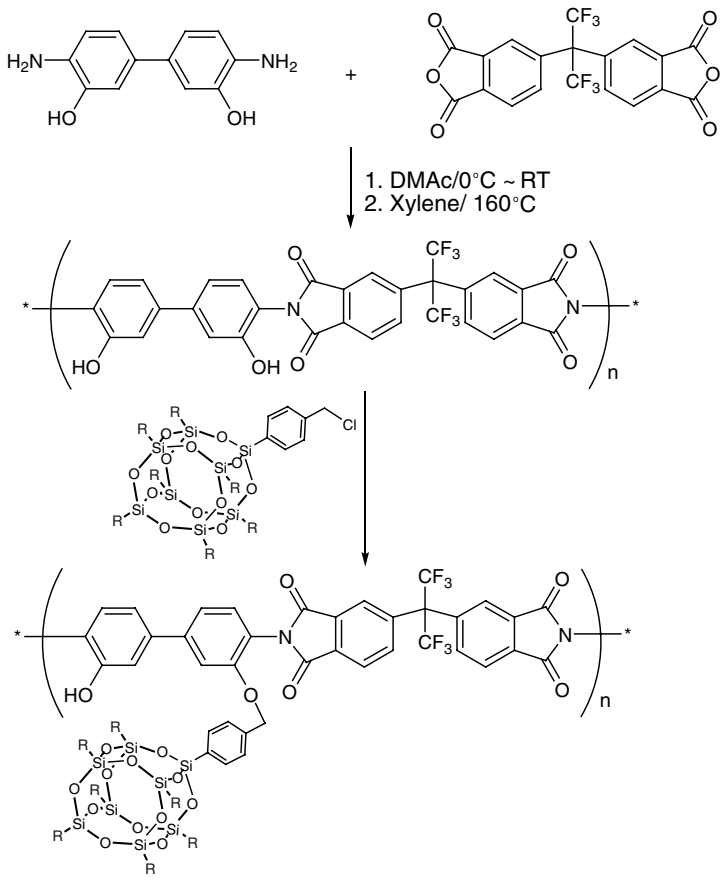

Figure 6.33 Polyimide-tethered POSS nanocomposites by grafting reaction.

epoxy-substituted POSS monomer was incorporated into an epoxy resin network composed of difunctional epoxies. The presence of POSS can increase the glass transition temperature of the epoxy resin because the nanoscopic size and mass of the POSS cages enhance their ability to hinder the segmental motion of molecular chains and network junctions. Chang et al. also reported a new nanomaterial (Figure 6.34) based on POSS-epoxy (OG) and *meta*-phenylenediamine (mPDA) [85]. The activation energy in curing the OG/mPDA system was higher than that of the DGEBA/mPDA system, as determined using both the Kissinger and Flynn–Wall–Ozawa methods [86, 87]. In an isothermal kinetic study based on an autocatalytic system, the activation energy for curing OG/mPDA was also higher than that of the DGEBA/mPDA system [85].

The T_g of the cured OG/mPDA product is significantly higher than that of the DGEBA/mPDA material because the presence of these POSS cages is able to effectively hinder the motion of the network junctions. The cured OG/mPDA product possesses inherently higher thermal stability than the cured DGEBA/mPDA product, as evidenced by the higher maximum decomposition temperature and the higher char yield of the former system. However, the existence of a large fraction of unreacted amino groups causes a lower initial decomposition temperature of the OG/mPDA system because

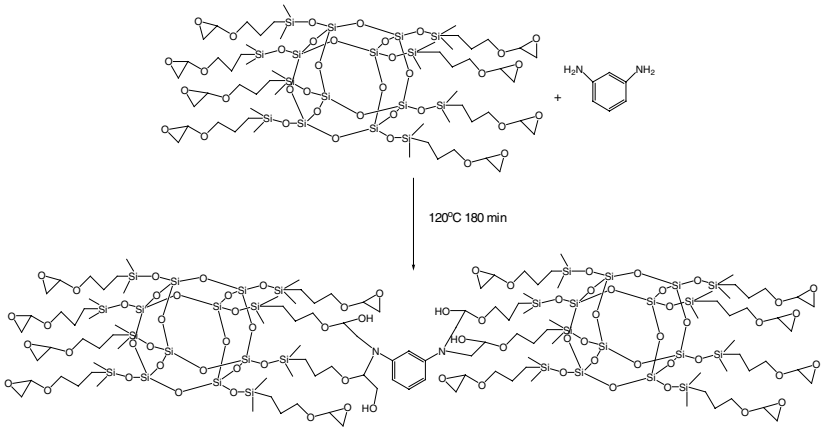

Figure 6.34 Curing mechanism of OG cured with mPDA.

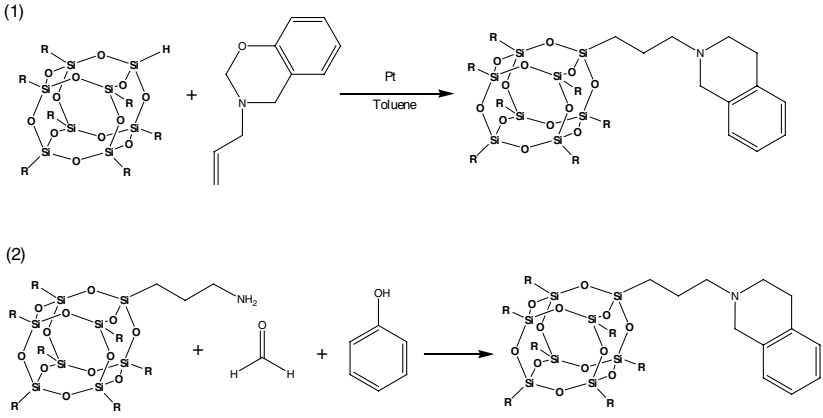

Figure 6.35 The chemical structure and mechanism for the synthesis of benzoxazine-POSS.

they tend to decompose or volatilize upon heating at relatively low temperatures. The dielectric constant of the OG/mPDA material (2.31) is substantially lower than that of the DGEBA/mPDA system (3.51) because of the presence of the nanoporous POSS cubes in the epoxy matrix [85].

6.4.8. Polybenzoxazine/POSS Nanocomposites

Chang et al. synthesized a novel benzoxazine ring containing POSS monomer (BZ–POSS) through two routes (Figure 6.35): (i) hydrosilylation of a vinyl-terminated benzoxazine using the hydrosilane functional group of a POSS derivative (H–POSS) and (ii) the reaction of a primary amine-containing POSS (amine-POSS) with phenol and formaldehyde [88]. The BZ–POSS monomer was copolymerized with other benzoxazine monomers through ring-opening polymerization under conditions similar to those used to polymerize pure benzoxazines. The thermal properties of these POSS-containing organic/inorganic polybenzoxazine nanocomposites were improved over those of the pure polybenzoxazine, as analyzed using DSC and TGA [88].

The chemical structure and mechanism for the synthesis of benzoxazine-POSS.

In addition, benzoxazine can be synthesized through the Mannich condensation of phenol, formaldehyde, and primary amines through ring-opening polymerization. Polybenzoxazines are phenolic-like materials that possess dimensional and thermal stability, and release no toxic byproducts during polymerization [89]. To further improve the thermal stability of polybenzoxazines, a hydrosilane-functionalized polyhedral oligomeric silsesquioxane (H-POSS) was incorporated into the vinyl-terminated benzoxazine monomer (VB-a) followed by ring-opening polymerization. Chang et al. also prepared hybrids from a nonreactive POSS (IB-POSS) and VB-a. The value of T_g of a regular polymerized VB-a (i.e., PVB-a) was 307°C, whereas for the hybrid containing 5 wt% H-POSS it was 333°C [90]. A new class of polybenzoxazine/POSS nanocomposites possessing network structures was prepared through reacting a multifunctional benzoxazine POSS (MBZ–POSS) with benzoxazine monomers (Pa and Ba) at various compositional ratios. The octafunctional cubic silsesquioxane (MBZ–POSS) used as the curing agent was synthesized from eight organic benzoxazine tethers through hydrosilylation of the vinyl-terminated benzoxazine monomer VP-a with Q_8M_8 using a Pt-dvs as the catalyst. Incorporation of the silsesquioxane cores into the polybenzoxazine matrix significantly hindered the mobility of the polymer chains and enhanced the thermal stability of these hybrid materials [90].

6.4.9. Other Applications

6.4.9.1. *Polymer Light Emitting Diodes (PLEDs) Incorporating POSS Hybrid Polymers*

Heeger et al. reported the incorporation of POSS moieties into conjugated polymers [91, 92], by synthesizing (Figure 6.36) the POSS-anchored semiconducting polymers POSS-

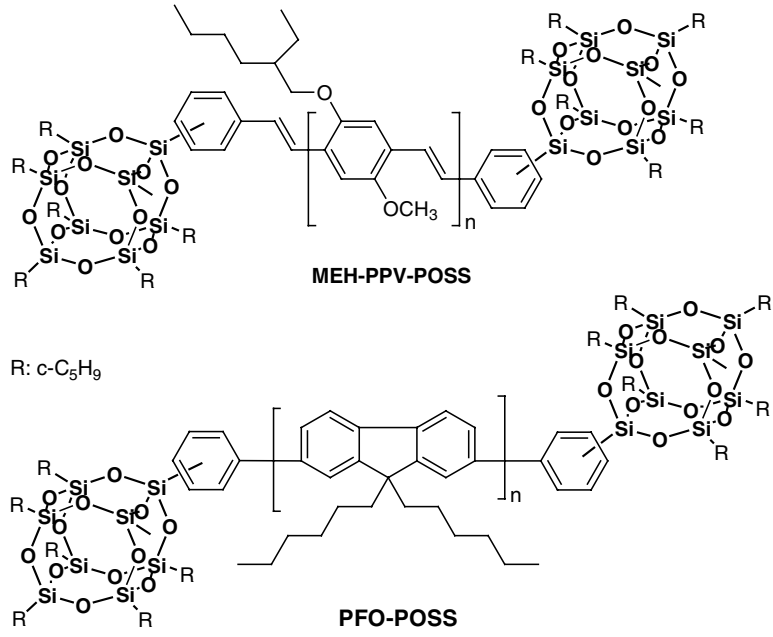

Figure 6.36 Molecular structure of MEH–PPV–POSS and PFO–POSS.

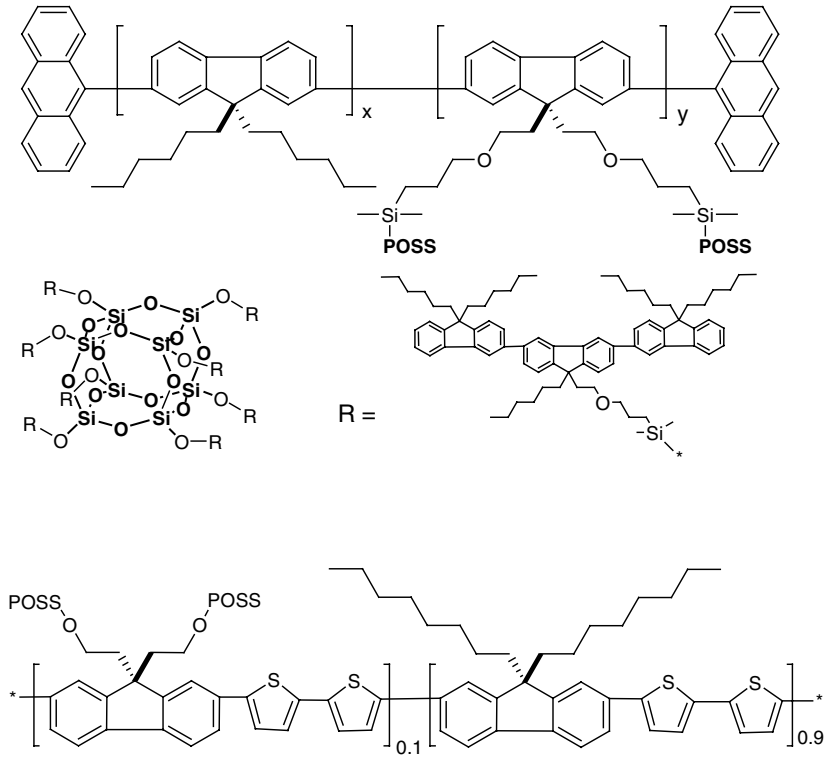

Figure 6.37 Molecular structure of PFO–POSS.

anchored poly(2-methoxy-5-(ethylexyloxy)-1,4-phenylenevinylene) (MEH–PPV–POSS) and POSS-anchored poly(9,9-dihexyfluorenyl-2,7-diyl) (PFO–POSS). Relative to the corresponding parent polymer, these POSS-anchored semiconducting polymers exhibited higher brightness and external quantum efficiencies [91, 92].

The role of POSS was suggested to reduce the formation of aggregation and/or excimers or to lower the concentration of conjugated defects. Shim et al. [93–96] prepared POSS-substituted polyfluorene polymers (Figure 6.37). The incorporation of the POSS groups inhibited interchain interactions and fluorenone formation and, thus, led to a reduction in the degree of undesired emission (>500 nm) of the poly(dialkylfluorene)s and an improvement in the thermal stability of the PFO–POSS systems. Devices incorporating PFO–POSS hybrids as emitting layers exhibited very stable blue light emissions and high performance [93].

Wei et al. and Hsu et al. [97–99] reported a new series of asymmetric conjugated polymers presenting POSS units on their side chains (Figure 6.38). An EL device prepared from MEH–PPV emitted a strong peak at 590 nm and a vibronic signal in the range 610–620 nm [97].

The introduction of bulky siloxane units into the PPV side chains presumably increases the interchain distance, thereby retarding interchain interactions and reducing the degree of exciton migration to defect sites. A star-like polyfluorene derivative, PFO–SQ, was synthesized through the Ni(0)-catalyzed reaction of octa(2-(4-bromophenyl) ethyl)octasilsesquioxane (OBPE–SQ) and polydioctylfluoroene (PFO), as depicted in Figure 6.39 [100]. The incorporation of the silsesquioxane core into the polyfluorene

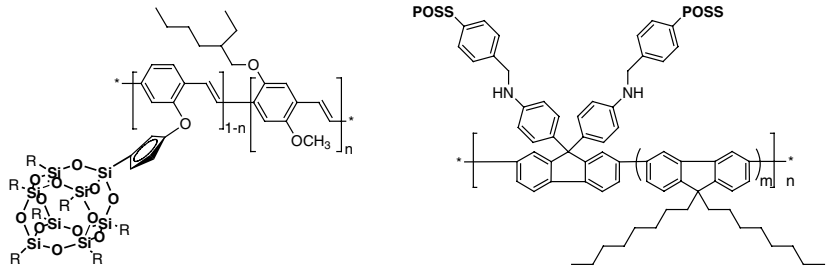

Figure 6.38 Synthesis of MEH–PPV–POSS.

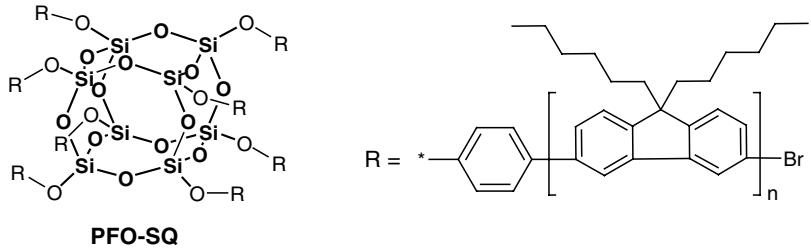

Figure 6.39 Synthetic route for PFO-SQ.

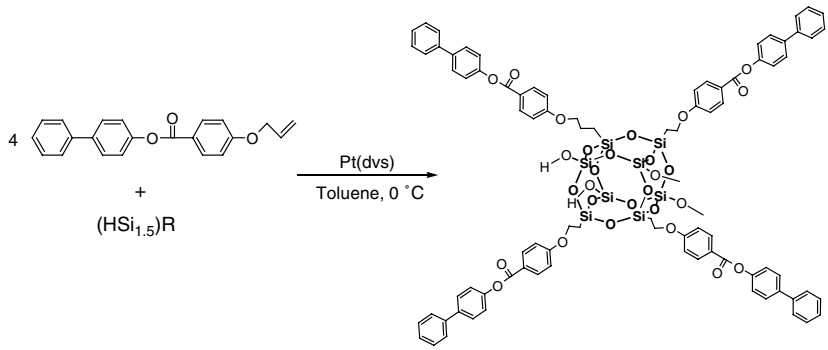

Figure 6.40 Syntheses of LC–POSS.

significantly reduced the degree of aggregation and enhanced the thermal stability. The incorporation of inorganic silsesquioxane cores into polyfluorenes is a new method for preparing organic light-emitting diodes with improved thermal and optoelectronic characteristics [100].

6.4.9.2. *Liquid Crystal Polymers (LCPs) Incorporating POSS Hybrid Polymers*

With the goal of developing diverse building blocks for nanocomposite materials, Laine and coworkers [101] synthesized liquid crystalline materials by appending mesogenic groups to cubic silsesquioxane cores via hydrosilylation of allyloxy-functionalized mesogens with octakis(dimethylsiloxy)octasilsesquioxane ($Q_8M_8^H$). Figure 6.40 indicates that hydrosilylation leads to cubes possessing an average of five appended LC groups; this

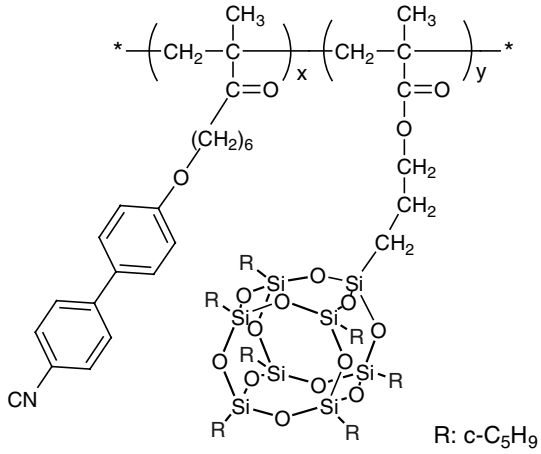

Figure 6.41 Synthesis of LC–POSS.

structure differs from the more "regular" fully LC-substituted analogs reported previously. Despite the structural irregularity, three of the four penta-LC-cube derivatives exhibited LC transitions, with a tendency to form SmA. One interesting observation was a redistribution of the diffuse liquid-like scattered intensity at 11–12 Å in the smectic phase upon alignment. These results provide the basis for future work on producing LC cubes as potential precursors to LC-ordered organic/inorganic nanocomposites. Although, the LC transition temperatures were reduced somewhat, they remained above those values considered useful for biologically important applications [101].

Chujo reported the preparation of a POSS macromonomer through radical copolymerization, LC hybrid copolymers incorporating various proportions of the synthesized LC monomer (Figure 6.41) [102]. The obtained LC hybrid polymers were soluble in common solvents, such as tetrahydrofuran, toluene, and chloroform. The thermal stability of the hybrid polymers increased upon increasing the ratio of POSS moieties [102].

6.4.9.3. *Lithographic Applications of POSS-Containing Photoresists*

Several POSS-based photoresists have been reported, including positive-tone POSS-containing photoresists. Wu et al. [103, 104] reported that the incorporation of POSS units in methacrylate-based chemically amplified photoresists influenced their reactive ion etching (RIE) behavior (Figure 6.42). Whereas polymers incorporating low POSS concentrations exhibited little improvements in their RIE resistances, the presence of 20.5 wt% POSS monomer in methacrylate-based resist significantly improved the RIE resistance in O_2 plasma. High-resolution transmission electron microscopy revealed that the RIE resistance improvement was due to the formation of rectangular crystallite-constituting networks of the silica cages uniformly distributed within the polymer matrix [103, 104].

Gonsalves et al. [105, 106] synthesized and characterized a series of POSS-containing positive-tone photoresists for use in both extreme ultraviolet lithography (EUVL) and electron beam lithography (Figure 6.43).

These photoresist systems exhibited the ideal combination of enhanced etch resistance and enhanced sensitivity required to satisfy both low- and high-voltage patterning applications. The photoresist sensitivity was enhanced after the direct incorporation of a

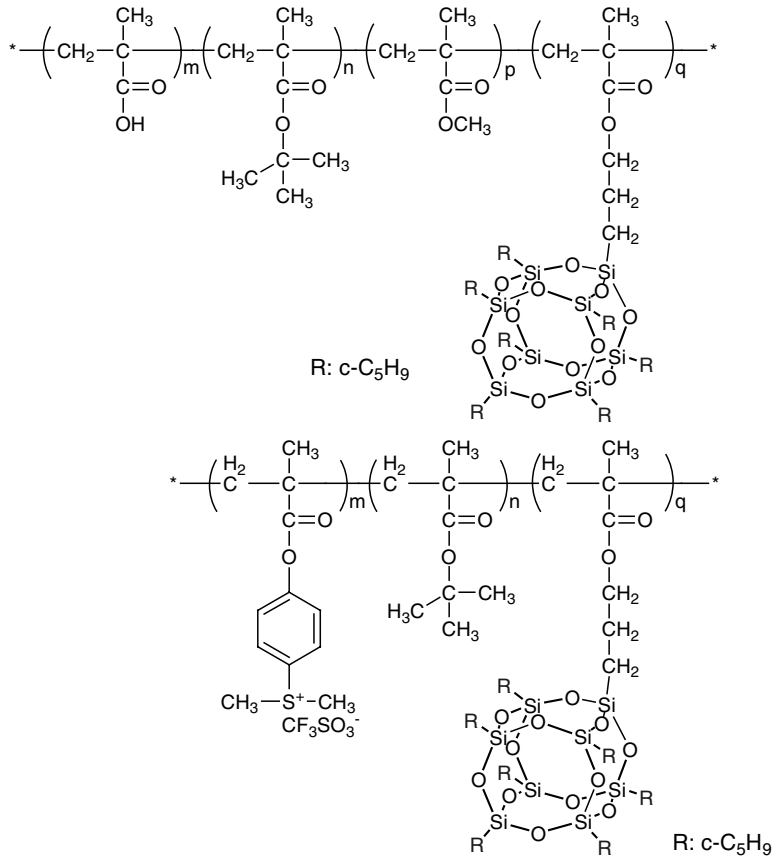

Figure 6.42 Microstructures of methacrylate-based chemically amplified photoresists.

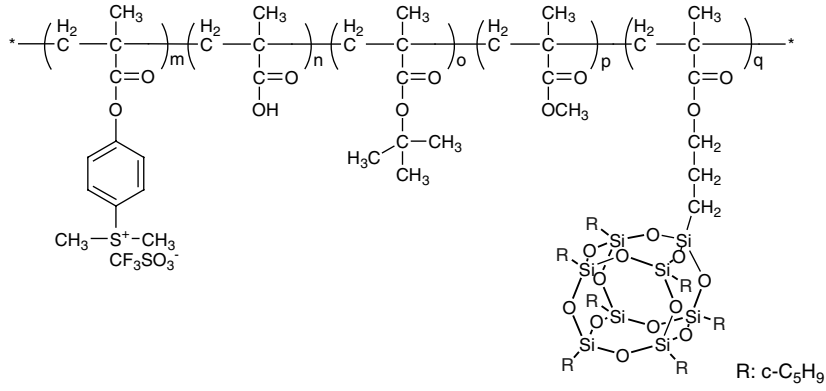

Figure 6.43 Microstructure of the nanocomposite resist.

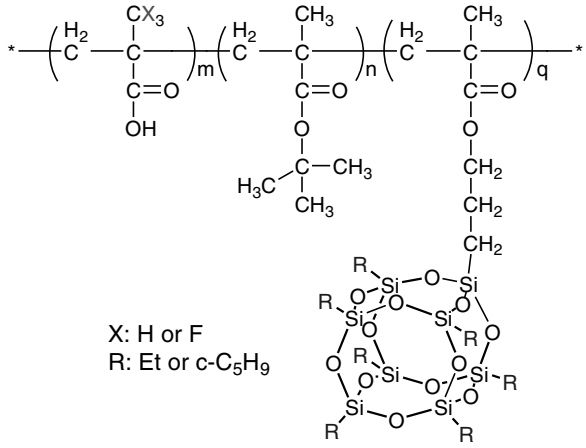

Figure 6.44 Microstructure of the POSS terpolymers.

photoacid-generating monomer into the resist polymer backbone, while the etch resistance of the material was improved after copolymerization with a POSS-containing monomer [105]. Argitis et al. [107–109] described the lithographic behavior and related material properties of chemically amplified, positive-tone, methacrylate-based photoresists incorporating POSS groups as the etch-resistant component (Figure 6.44).

The POSS-containing photoresists studied for 157-nm lithographic applications exhibited high sensitivity (<10 mJ/cm^2 under open field exposure), no silicon outgassing, and sub-100-nm resolution capabilities; indeed, 90-nm patterns in 100-nm-thick films could be resolved. Alternatively, an octavinylsesquioxane dry resist was prepared as a negative-tone resist that exhibited high sensitivity for deep-UV, electron-beam, and X-ray lithography [110]. Furthermore, Zheng et al. [111] synthesized a novel photosensitive otaccinnamoylamidophenyl POSS derivative (OcapPOSS) through the reaction of cinnamoyl chloride and octaaminophenyl POSS. The presence of the POSS cages restricted the mobility of the poly(vinyl cinnamate) macromolecular chains and, thus, hindered the formation of tetrabutane rings. DSC analysis revealed that the values of T_g of the nanocomposites were significantly higher than that of the parent poly(vinyl cinnamate). Recently, Chang et al. [112] developed methacrylate-based, POSS derivative-containing photoresist materials for UV-lithography with enhanced sensitivity, higher contrast, and improved resolution as a result of the presence of hydrogen bonding interactions between the siloxane units of the POSS moieties and the OH groups [30, 39]. Hydrogen bonding interactions within these photosensitive copolymers not only formed physically crosslinked bonds but also raised the density of methacrylate olefinic units around the POSS moieties, thereby enhancing the rate of chemically crosslinked photopolymerization (Figure 6.45) [112].

6.4.9.4. *Low-k Applications of POSS-Containing Materials*

To decrease the dielectric constants of polymers, several research groups [113–117] have been exploring the possibility of incorporating various nanoforms into polymer matrixes to take the advantage of the low dielectric constant of air (k = 1). There are two typical routes employed for preparing materials with low dielectric constants: (i) nanopore formation through decomposition (e.g., thermal decomposition, photodegradation with UV irradiation, or solvent etching) of a dispersion phase within a material matrix and

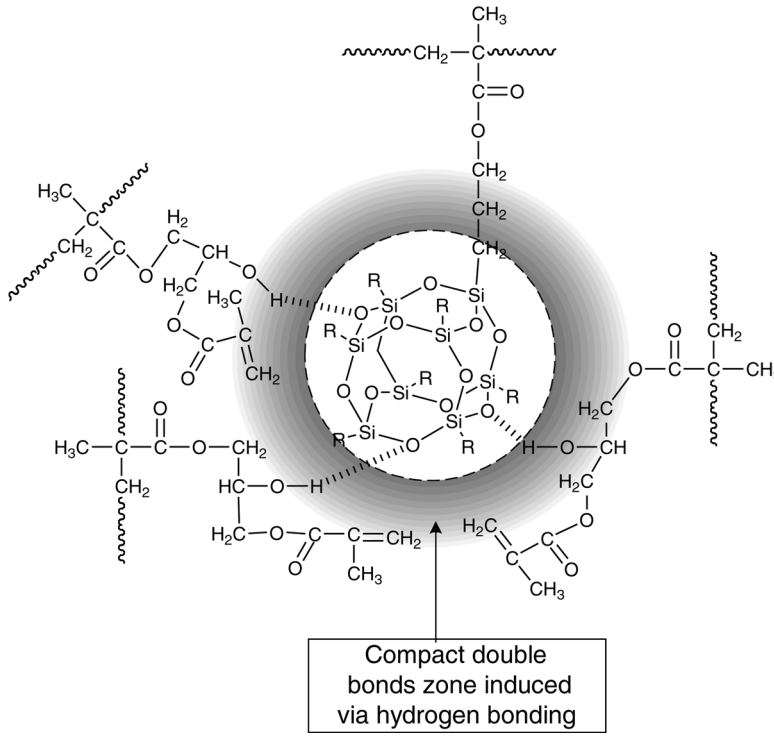

Figure 6.45 The proposed microstructure via hydrogen bonding interaction of POSS.

(ii) incorporation of a low-*k* moieties (e.g., fluorinated units, supercritical fluids, or low-*k* particles) within a material matrix. There are several drawbacks to each of these two methods, such as contaminant release, solvent effects, and compatibility of the dispersion and the matrix. Recently, a low dielectric constant material was prepared after dispersion of POSS-containing molecules into a polymer matrix [51, 53]. Chang et al. developed some POSS-containing low-*k* materials using both of the methods mentioned above, taking advantage of hydrogen bonding interactions between the POSS moieties and OH groups to achieve homogenous nanocomposites [118, 119]. In these nanocomposite materials, the POSS moieties not only served as low-*k* materials but also contributed to the improved thermal and mechanical properties.

6.5. Conclusion

The POSS nanocomposites presented here are composite materials reinforced with silica cages, i.e., an ultrafine filler of nanometer size, which is almost equal to the size of the polymer matrix. Although the POSS content can be as low as ca. 1–5 wt%, individual POSS particles can exist at distances as close as several nanometers apart. Therefore, these nanocomposites possess microstructures that do not exist in conventional composites. For this reason, the field of POSS nanocomposite research has become extremely active in recent years (Figure 6.46). In this chapter, we have reviewed only the studies that have made major contributions to this research field, focusing on the preparation of such polymer–POSS nanocomposites as styryl-POSS, methacrylate-POSS,

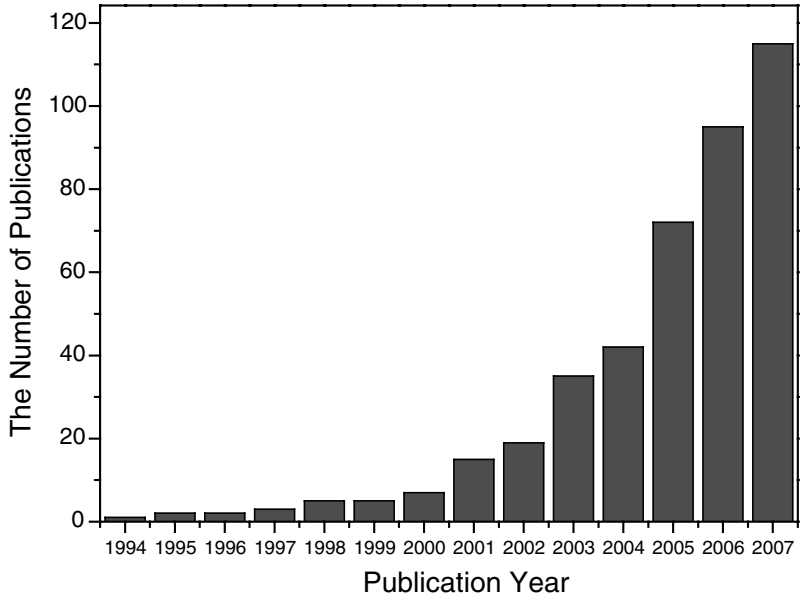

Figure 6.46 Statistics of POSS publications during recent years.

norbornyl-POSS, vinyl-POSS, epoxy-POSS, phenolic-POSS, benzoxazine-POSS, amine-POSS, and hydroxyl-POSS. Both monofunctional and multifunctional monomers of these types are used to prepare commercial and/or high-performance thermoplastic and thermosetting polymers. This chapter also provides details of their corresponding thermal, dynamic mechanical, electrical, and surface properties. Other important publications related to POSS are cited in the reference section [120–161].

Acknowledgments

This work was supported financially by the National Science Council, Taiwan, Republic of China, under Contract No. NSC-96-2120-M-009-009 and NSC-96-2218-E-110-008 and Ministry of Education "Aim for the Top University" program (MOEATU program).

References

1. Li, G.; Wang, L.; Ni, H.; Pittman Jr. C. U. *J. Inorgan. Organometal. Polym.* **2001**, 3, 123.
2. Scott, D. W. *J. Am. Chem. Soc.* **1946**,68, 356.
3. Baney, R. H.; Itoh, M.; Sakakibara, A.; Suzuki, T. *Chem. Rev.* **1995**, 95, 1409.
4. Gozdz, A. S. *Polym. Adv. Technol.* **1994**, 5, 70.
5. Voronkov, M. G.; Lavrentyev, V. I. *Topics Curr. Chem.* **1982**, 102, 199.
6. Feher, F. J.; Terroba, R.; Jin, R.; Wyndham, K. O.; Lucke, S.; Brutchey, R.; Nguyen, F. *Polym. Mater. Sci. Eng.* **2000**,82, 301.
7. Brown, I. F. *New Sci.* **1963**, 17, 304.
8. Martynova, T. N.; Chupakhina, T. I. *J. Organometal. Chem.* **1988**,345, 11.
9. Agaskar, P. A. *Inorg. Chem.* **1991**,30, 2707.
10. Chalk, A. J.; Harrod, J. F. *J. Am. Chem. Soc.* **1965**,87, 16.
11. Tsuchida, A.; Bolln, C.; Sernetz, F. G.; Frey, H.; Mulhaupt, R. *Macromolecules* **1997**,30, 2818.
12. Calzaferri, G.; Herren, D.; Imhof, R. *Helv. Chim. Acta* **1991**,74, 1278.

13. Calzaferri, G.; Imhof, R. *J. Chem. Soc., Dalton Trans.* **1992**, 3391.
14. Marcolli, C.; Imhof, R.; Calzaferri, G. *Microchim. Acta* **1997**,14, 493.
15. Feher, F. J. *J. Am. Chem. Soc.* **1986**, 108, 3850.
16. Feher, F. J.; Weller, K. J. *Organometal.* **1990**, 9, 2638.
17. Feher, F. J.; Weller, K. J . *Inorg. Chem.* **1991**, 30, 880.
18. Feher, F. J.; Newman, D. A.; Walzer, J. F. *J. Am. Chem. Soc.* **1989**,111, 1741.
19. Lichtenhan, J. D. *Comments Inorg. Chem.* **1995**,17, 115 .
20. Ruffieux, V.; Schmid, G.; Braunstein, P.; Rose, J. *Chem. Eur. J.* **1997**,3, 900.
21. Murugavel, R.; Voigt, A.; Walawalkar, M. G.; Roesky, H. W. *Chem. Rev.* **1996**,96, 2205.
22. Feher, F. J.; Budzichowski, T. A.; Weller, K. J. *J. Am. Chem. Soc.* **1989**,111, 7288.
23. Feher, F. J.; Budzichowski, T. A.*Organometal.* **1991**,10, 812.
24. Feher, F. J.; Walzer, J. F. *Inorg. Chem.* **1991**,30, 1689.
25. Frye, C. L.; Collins, W. T. *J. Am. Chem. Soc.* **1970**,92, 5586.
26. Zhang, C.; Laine, R. M. *J. Am. Chem. Soc.* **2000**, 122, 6979.
27. Sellinger, A.; Laine, R. M. *Macromolecules* **1996**, 29, 2327.
28. Sellinger, A.; Laine, R. M. *Chem. Mater.***1996**, 8, 1592.
29. Painter, P. C.; Coleman, M. C. *Prog. Polym. Sci.* **1995**, 20, 1.
30. Lee. Y. J.; Kuo, S. W.; Huang, W. J. Lee, H. Y. Chang, F. C. *J. Polym. Sci. Polym. Sci. Ed.* **2004**, 42, 1127.
31. Noda, I. *J. Am. Chem. Soc.* **1989**, 111, 8116.
32. Coggesthall, N.D.; Saier, E. L. *J. Am. Chem. Soc.* **1951**, 71, 5414.
33. Wu, H. D.; Chu, P. P.; Ma, C. C. M.; Chang, F.C. *Macromolecules* **1999**, 32, 3097.
34. Kuo, S. W. Lin, H. C. Huang, W. J. Huang, C. F. Chang, F. C. *J. Polym. Sci. Polym. Sci. Ed.* **2006**, 44, 673.
35. Moskala, E. J.; Varnell D. F.; Coleman, M. M. *Polymer*, **1985**, 26, 228.
36. Kuo, S. W. ; Chang, F. C. *Macromol. Chem. Phys.* **2002**, 203, 868.
37. Kwei, T. K. *J. Polym. Sci., Polym. Lett. Ed.*, **1984**,22, 307.
38. Huang, C. F.; Kuo, S. W.; Chen, Y. K.; Chang, F. C. *Polymer* **2004**, 45, 5913.
39. Lin, H. C.; Kuo, S. W. Huang, C. F. Chang, F. C. *Macromol. Rapid Commun.* **2006**, 27, 537.
40. Fu, B. X.; Yang, C.; Somani, R. H. Zong, S. X.; Hsiao, B. S.; Phillips, S.; Blanski, R.; Ruth, D. *J. Polym. Sci. Polym. Sci. Ed.* **2001**,39, 2727.
41. Fina, A.; Tabuani, D.; Frache, A.; Camino, G. *Polymer* **2005**, 46, 7855.
42. Pracella, M.; Chionna, D.; Fina, A.; Tabuani, D.; Frache, A.; Camino, G. *Macromol. Symp.* **2006**, 234, 59.
43. Zheng, L.; Farris, R. J.; Coughlin, E. B. *Macromolecules* **2001**,34, 8034.
44. Zheng, L.; Farris, R. J.; Coughlin, E. B. *J. Polym. Sci.: Part A: Polym. Chem.* **2001**, 39, 2920.
45. Mather, P. T.; Jeon, H. G.; Uribe, A. R. *Macromolecules* **1999**, 32, 1194.
46. Haddad, T. S.; Lichtenhan, J. D. *Macromolecules* **1996**, 29, 7302.
47. Zheng, L.; Kasi, R. M.; Farris, R. J.; Coughlin, E. B. *J. Polym. Sci.: Part A: Polym. Chem. Ed* .**2002**, 40, 885.
48. Cardoen, G.; Coughlin, E. B. *Macromolecules* **2004**, 37, 5123.
49. Xu, H.; Kuo, S. W.; Huang, C. F.; Chang, F. C. *J. Polym. Res.* **2002**, 9, 239.
50. Xu, H.; Kuo, S. W.; Lee, J. S.; Chang, F. C. *Macromolecules* **2002**, 35, 8788.
51. Xu, H.; Kuo, S. W.; Chang, F. C. *Polym. Bull.* **2002**, 48, 869.
52. Xu, H.; Kuo, S. W.; Lee, J. S.; Chang, F. C. *Polymer* **2002**, 43, 5117.
53. Lichtenhan, J. D.; Otonari, Y. A.; Carr, M. J. *Macromolecules* **1995**, 28, 8435.
54. Kopesky, E. T.; Haddad, T. S.; Cohen, R. E.; Mckinley, G. H. *Macromolecules* **2004**, 37, 8992.
55. Li, G. Z.; Cho, H.; Wang, L.; Toghiani, H.; Pittman Jr. C. *J. Polym. Sci.: Polym. Chem. Ed.* **2005**, 43, 355.
56. Bizet, S.; Galy, J.; Gerard, J. F. *Macromolecules* **2006**, 39, 2574.
57. Kopesky, E. T.; McKinley, G. H.; Cohen, R. E. *Polymer* **2006**, 47, 299.
58. Castelvetro, V.; Ciardelli, F.; Vita, C. D.; Puppo A. *Macromol. Rapid Commun.* **2006**, 27, 619.
59. Patel, R. R.; Mohanraj, R.; Pittman Jr. C. U. *J. Polym. Sci.: Polym. Phy. Ed.* **2006**, 44, 234.
60. Pyun, J.; Matyjaszewski, K. *Macromolecules* **2000**, 33, 217.
61. Pyun, J.; Matyjaszewski, K. *Polymer* **2003**, 44, 2739.
62. Chen, R.; Feng, W.; Zhu, S.; Botton, G.; Ong, B.; Wu, Y. *Polymer* **2006**, 47, 1119.
63. Costa, R. O. R.; Vasconcelos, W. L.; Tamaki, R.; Laine, R. M. *Macromolecules* **2001**; 34; 5398.
64. Ohno, K.; Sugiyama, S.; Koh, K.; Tsujii, Y.; Fukuda, T.; Yamahiro, M.; Oikawa, H.; Yamamoto, Y.; Ootake, N.; Watanabe, K. *Macromolecules* **2004**, 37, 8517.
65. Koh, K.; Sugiyama, S.; Morinaga, T.; Ohno, K.; Tsujii, Y.; Fukuda, T.; Yamahiro, M.; Iijima, T.; Oikawa, H.; Watanabe, K.; Miyashita, T. *Macromolecules* **2005**, 38, 1264.

66. Huang, C. F.; Kuo, S. W.; Lin, F. J.; Huang, W. J.; Wang, C. F.; Chen, W. Y.; Chang, F. C. *Macromolecules* **2006**; 39; 300.
67. Maitra, P.; Wunder, S. L. *Chem. Mater.* **2002**, 14, 4494.
68. Kim, B. S.; Mather, P. T. *Macromolecules* **2002**, 35, 8378.
69. Chan, S. C.; Kuo, S. W.; Chang, F. C. *Macromolecules* **2005**, 38, 3099
70. Liu, Y. H.; Yang, X. T.; Zhang, W. A.; Zheng, S. X. *Polymer* **2006**, 47, 6814.
71. Laine, R. M.; Tamaki, R.; Choi, J.; Brick, C.; Kim, S. G. *Organic/Inorganic Hybrid Materials Workshop*. Sonoma, CA: ACS, 2000.
72. Tamaki, R.; Choi, J.; Laine, R. M. *Chem. Mater.* **2003**, 15, 793.
73. Olsson, K.; Gronwall, C. *Arkiv. Kemi.* **1961**, 17, 529.
74. Huang, J.; Xiao, Y.; Mya, K. Y.; Liu, X.; He, C.; Dai, J.; Siow, Y. P. *J. Mater. Chem.* **2004**, 14, 2858.
75. Lee, Y. J.; Huang, J. M.; Kuo, S. W.; Lu, J. S.; Chang, F. C. *Polymer* **2005**, 46, 173.
76. Leu, C. M.; Chang, Y. T.; Wei, K. H. *Macromolecules* **2003**, 36, 9122.
77. Leu, C. M.; Reddy, G. M.; Wei, K. H.; Shu, C. F. *Chem. Mater.* **2003**, 15, 2261.
78. Leu, C. M.; Chang, Y. T.; Wei, K. H. *Chem. Mater.* **2003**, 15, 3721.
79. Choi, J.; Harcup, J.; Yee, A. F.; Zhu,Q.; Laine, R. M. *J. Am. Chem. Soc.* **2001**, 123, 11240.
80. Liu, Y. L.; Chang, G. P. *J. Polym. Sci.: Polym. Chem. Ed.* **2006**, 44, 1869.
81. Liu, Y.; Zheng, S.; Nie, K. *Polymer* **2005**, 46, 12016.
82. Huang, J.; He, C.; Liu, X.; Xu, J.; Tay, C. S. S.; Chow, S. Y. *Polymer* **2005**, 46, 7018.
83. Strachota, A.; Kroutilova, I.; Rova, J. K.; Matejka, L. *Macromolecules* **2004**, 37, 9457.
84. Abad, M. J.; Barral, L.; Fasce, D. P.; Williams, R. J. J. *Macromolecules* **2003**, 36, 3128.
85. Chen, W. Y.; Wang, Y. Z.; Kuo, S. W.; Huang, C. F.; Tung, P. H.; Chang, F. C. *Polymer* **2004**, 45, 6897.
86. Kissinger, H. E. *Anal. Chem.* **1957**, 29, 1702.
87. Ozawa T. *Bull. Chem. Soc. Jpn.* **1965**, 38, 1881.
88. Lee, Y. J.; Kuo, S. W.; Su, Y. C.; Chen, J. K.; Tu, C. W.; Chang, F. C. *Polymer* **2004**, 45, 6321.
89. Lee, Y. J.; Huang, J. M.; Kuo, S. W.; Chen, J. K. Chang, F. C. *Polymer* **2005**, 46, 2320.
90. Lee, Y. J.; Kuo, S. W.; Huang, C. F.; Chang, F. C. *Polymer* **2005**, 47, 4378.
91. Xiao, S.; Nguyen, M.; Gong, X.; Cao, Y.; Wu, H.; Moses, D.; Heeger, A. J. *Adv. Funct. Mater.* **2003**, 13, 25.
92. Gong, X.; Soci, C.; Yang, C. Y.; Heeger, A. J.; Xiao, S. *J. Phys. D: Appl. Phys.* **2006**, 39, 2048.
93. Lee, J.; Cho, H.; Jung, B.; Cho, N.; Shim, H. *Macromolecules* **2004**,37, 8523.
94. Cho, H. J.; Hwang, D. H.; Lee, J. I.; Yung, Y. K.; Park, J. H.; Lee, J.; Lee, S. K.; Shim, H. K. *Chem. Mater.* **2006**, 18, 3780.
95. Lee, J.; Cho, H. J.; Cho, N. S.; Hwang, D. H.; Kang, J. M.; Lim, E.; Lee, J. I.; Shim, K. H. *J. Polym. Sci.: Part A: Polym. Chem.* **2006**, 44, 2943.
96. Kang, J. M.; Cho, H. J.; Lee, J.; Lee, J. I.; Lee, S. K.; Cho, N. S.; Hwang, D. H.; Shim, H. K. *Macromolecules* **2006**, 39, 4999.
97. Chen, K. B.; Chen, H. Y.; Yang, S. H.; Hsu, C. S. *J. Polym. Res.* **2006**, 13, 229.
98. Chou, C. H.; Hsu, S. L.; Yeh, S. W.; Wang, H. S.; Wei, K. H. *Macromolecules* **2005**,38, 9117.
99. Chou, C. H.; Hsu, S. L.; Dinakaran, K.; Chiu, M. Y.; Wei, K. H. *Macromolecules* **2005**,38, 745.
100. Lin, W. J.; Chen, W. C.; Wu, W. C.; Niu, Y. H.; Jen, A. K. J. *Macromolecules* **2004,** 37,2335.
101. Zhang, C.; Bunning, T. J.; Laine, R. M. *Chem. Mater.* **2001**, 13, 3653.
102. Kim, K. M.; Chujo, Y. *J. Polym. Sci.: Part A: Polym. Chem.* **2001**, 39, 4035.
103. Wu, H.; Hu, Y.; Gonsalves, K. E.; Yacaman, M. J. *J. Vac. Sci. Technol. B.* **2001**, 19, 851.
104. Wu, H.; Gonsalves, K. E. *Adv. Mater.* **2001**, 13, 670.
105. Ali, M. A.; Gonsalves, K. E.; Golovkina, V.; Cerrina, F. *Microelectron. Eng.* **2003**, 65, 454.
106. Ali, M. A.; Gonsalves, K. E.; Agrawal, A.; Jeyakumar, A.; Henderson, C. L. *Microelectron. Eng.* **2003**, 70, 19.
107. Bellas, V.; Tegou, E.; Raptis, I.; Gogolides, E.; Argitis, P.; Iatrou H.; Hadjichristidis, N.; Sarantopoulou, E.; Cefalas, A. C. *J. Vac. Sci. Technol. B* **2002**, 20, 2902.
108. Tegou, E.; Bellas, V.; Gogolides, E.; Argitis, P.; Eon, D.; Cartry, G.; Cardinaud, C. *Chem. Mater.* **2004**, 16, 2567.
109. Tegou, E.; Bellas, V.; Gogolides, E.; Argitis, P. *Microelectron. Eng.* **2004**, 73, 238.
110. Schmidt, A.; Babin, S.; Koops, H. W. P. *Microelectron. Eng.* **1997**, 35, 129.
111. Ni, Y.; Zheng, S. *Chem. Mater.* **2004**,16, 5141.
112. Lin, H. M.; Wu, S. Y.; Huang, C. F.; Kuo, S. W.; Chang, F. C. *Macromol. Rapid Commun.* **2006**, 27, 1550.
113. Carter, K. R.; McGrath, J. E. *Chem. Mater.* **1997**, 9, 105.

114. Carter, K. R.; DiPietro, R. A.; Sanchez, M. I.; Swanson, S. A. *Chem. Mater.* **2001**, 13, 213.
115. Mikoshiba, S.; Hayase, S. *J. Mater. Chem.* **1999**, 9, 591.
116. Krause, B. R.; Mettinkhof; N. F. *Macromolecules* **2001**, 34, 874.
117. Krause, B. R.; Mettinkhof, N. F. *Adv. Mater.* **2002**, 14, 1041.
118. Lee, Y. J.; Huang, J. M.; Kuo, S. W.; Chang, F. C. *Polymer* **2005**, 46, 10056.
119. Chen, W. Y.; Ho, K, S.; Hsieh, T. H.; Chang, F. C.; Wang, Y. Z. *Macromol. Rapid Commun.* **2006**, 27, 452.
120. Haddad, T. S.; Lichtenhan, J. D. *J. Inorgan. Organometal. Polym.* **1995**, 5, 237.
121. Mantz, R. A.; Jones. P. F.; Chaffee; K. P.; Lichtenhan; J. D.; Gilman; J. W.; Ismail; I. M. K; Burmeister, M. J. *Chem. Mater.* **1996**, 8, 1250.
122. Romo-Uribe A.; Mather, P. T.; Haddad, T. S.; Lichtenhan, J. D. *J. Polym. Sci.: Polym. Phys. Ed.* **1998**, 36, 1857.
123. Lee, A.; Lichtenhan, J. D. *Macromolecules* **1998**, 31, 4970.
124. Mather, P. T.; Jeon, H. G.; Romo-Uribe, A.; Haddad, T. S.; Lichtenhan, J. D. *Macromolecules* **1999**, 32, 1194.
125. Shockey, E. G.; Bolf, A. G.; Jones, P. F.; Schwab, J. J.; Chaffee, K. P.; Haddad, T. S.; Lichtenhan, J. D. *Appl. Organometall. Chem.* **1999**, 13, 311.
126. Bharadwaj, R. K.; Berry, R. J.; Farmer, B. L. *Polymer* **2000**, 41, 7209.
127. Fu, B. X.; Hsiao, B. S.; Pagola, S.; Stephens, P.; White, H.; Rafailovich, M.; Sokolov, J.; Mather, P. T.; Jeon, H. G.; Phillips, S.; Lichtenhan, J.; Schwab, J. *Polymer* **2001**,42, 599.
128. Zheng, L.; Farris, R. J.; Coughlin, E. B. *J. Polym. Sci.: Polym. Chem. Ed.* **2001**, 39, 2920.
129. Kim, K. M.; Chujo, Y. *J. Polym. Sci.: Polym. Chem. Ed.* **2001**, 39, 4035.
130. Zheng, L.; Farris, R. J.; Coughlin, E. B. *Macromolecules* **2001**, 34, 8034.
131. Li, G. Z.; Wang, L. C.; Toghiani, H.; Daulton, T. L.; Koyama, K.; Pittman, C. U. *Macromolecules* **2001**, 34, 8686.
132. Zheng, L.; Waddon, A. J.; Farris, R. J.; Coughlin, E. B. *Macromolecules* **2002**, 35, 2375.
133. Zhang, W. H.; Fu, B. X.; Seo, Y.; Schrag, E.; Hsiao, B.; Mather, P. T.; Yang, N. L.; Xu, D. Y.; Ade, H.; Rafailovich, M.; Sokolov, J. *Macromolecules* **2002**, 35, 8029.
134. Waddon, A. J.; Zheng, L.; Farris, R. J.; Coughlin, E. B. *Nano Lett.* **2002**, 2, 1149.
135. Abad, M. J. Barral, L.; Fasce, D. P.; Williams, R. J. J. *Macromolecules* **2003**, 36, 3128.
136. Huang, J. C.; He, C. B.; Xiao, Y.; Mya, K. Y.; Dai, J.; Siow, Y. P. *Polymer* **2003**, 44, 4491.
137. Carroll, J. B.; Waddon, A. J.; Nakade, H.; Rotello, V. M. *Macromolecules* **2003**, 36, 6289.
138. Lamm, M. H.; Chen, T.; Glotzer, S. C. *Nano Lett.* **2003**, 3, 989.
139. Waddon, A. J.; Coughlin, E. B. *Chem. Mater.* **2003**, 15, 4555.
140. Huang, J. C.; Li, X.; Lin, T. T.; He, C. B.; Mya, K. Y.; Xiao, Y.; Li, J. *J. Polym. Sci.: Polym. Phy. Ed.* **2004**, 42, 1173.
141. Yei, D. R.; Kuo, S. W.; Su, Y. C.; Chang, F. C. *Polymer* **2003**, 45, 2633.
142. Baker, E. S.; Gidden, J.; Anderson, S. E.; Haddad, T. S.; Bowers, M. T. *Nano Lett.* **2004**, 4, 779.
143. Fu, B. X.; Lee, A.; Haddad, T. S. *Macromolecules* **2004**, 37, 5211.
144. Dvornic, P. R.; Hartmann-Thompson, C.; Keinath, S. E.; Hill, E. J. *Macromolecules* **2004**, 37, 7818.
145. Zheng, L.; Hong, S.; Cardoen, G.; Burgaz, E.; Gido, S. P.; Coughlin, E. B. *Macromolecules* **2004**, 37, 8606.
146. Liu, H. Z.; Zhang, W.; Zheng, S. X. *Polymer* **2005**, 46, 157.
147. Liu, H. X.; Zheng, S. X. *Macromol. Rapid Commun.* **2005**, 26, 196.
148. Anderson, S. E.; Baker, E. S.; Mitchell, C.; Haddad, T. S.; Bowers, M. T. *Chem. Mater.* **2005**, 17, 2537.
149. Turri, S.; Levi, M. *Macromolecules* **2005**, 38, 5569.
150. Liu, Y. H.; Meng, F. L.; Zheng, S. X. *Macromol. Rapid Commun.* **2005**, 26, 920.
151. Hillson, S. D.; Smith, E.; Zeldin, M.; Parish, C. A. *Macromolecules* **2005**, 38, 8950.
152. Xu, H. Yang, B.; Wang, J. Guang, S.; Li, C. Li, C. *Macromolecules* **2005**, 38, 10455.
153. Joshi, M.; Butola, B. S.; Simon, G.; Kukaleva, N. *Macromolecules* **2006**, 39, 1839.
154. Bizet, S.; Galy, J.; Gerard, J. F. *Macromolecules* **2006**, 39, 2574.
155. Soong, S. Y.; Cohen, R. E.; Boyce, M. C.; Mulliken, A. D. *Macromolecules* **2006**, 39, 2900.
156. Cui, L.; Zhu, L. *Langmuir* **2006**, 22, 5982.
157. Cui, L.; Collet, J. P.; Xu. G. Q.; Zhu, L. *Chem. Mater.* **2006**, 18, 3503.
158. Miao, J. J.; Cui, L.; Lau, H. P.; Mather, P. T.; Zhu, L. *Macromolecules* **2007**, 40, 5460.
159. Ni, Y.; Zheng, S. X. *Macromolecules* **2007**, 40, 7009.
160. Hao, N.; Boehning, M.; Schoenhals A. *Macromolecules* **2007**, 40, 9672.
161. Markovic, E.; Ginic-Markovic M.; Clarke, S.; Matisons, J.; Hussain, M.; Simon, G. P. *Macromolecules* **2007**, 40, 2694.